(NASA-CR-177228) SUBLAMINATE ANALYSIS OF INTERLAMINAR FRACTURE IN COMPOSITES Final Technical Report (Georgia Inst. of Tech.) 89 p HC A05/MF A01 CSCL 11D

N86-28130

G3/24 Unclas 43394

SUBLAMINATE ANALYSIS OF INTERLAMINAR FRACTURE IN COMPOSITES *

Erian A. Armanios and Lawrence W. Rehfield **
School of Aerospace Engineering
Georgia Institute of Technology
Atlanta, Georgia 30332 USA
(404) 894-3067

Abstract

A simple analysis method based upon a transverse shear deformation theory and a sublaminate approach is utilized to analyze a Mixed-Mode edge delamination specimen. The analysis provides closed form expressions for the interlaminar shear stresses ahead of the crack, the total energy release rate, and the energy release rate components. The parameters controlling the behavior are identified. The effect of specimen stacking sequence and delamination interface on the strain energy release rate components is investigated. Results are compared with a finite element simulation for reference. The simple nature of the method makes it suitable for preliminary design analyses which require a large number of configurations to be evaluated quickly and economically.

---

* *This work was sponsored by the NASA Langley Research Center under Grant* NAG-1-558.

** Research Engineer and Professor, respectively.

Introduction

Delaminations along the free edges of laminates subjected to tensile loading have been observed during testing and service. The presence of delamination, initiated by interlaminar stresses, causes redistribution of the stresses among plies in a laminate and, therefore, usually results in a reduction of stiffness and strength. The edge delamination (ED) test has been proposed by Pagano and Pipes[1] to characterize the interlaminar peel strength of laminated composite materials. O'Brien[2] extended the scope of the test to investigate delamination onset and growth in graphite/epoxy laminates under uniform extension. A simple expression was also developed for the total energy release rate. The energy release rate components G_I, G_{II} and G_{III} associated with the opening, shearing and tearing modes, respectively, were estimated based on a finite element simulation and the crack-closure method[2,3].

A similar approach was used to study delaminations around an open hole in composite laminates[4]. Discrete locations around the hole boundary were modeled as straight edges, with the ply orientations rotated by an appropriate angle. Delamination was found to be governed by the percentage of Mode I for a given geometry under static loading for the graphite/epoxy material systems under consideration.

Whitney and Knight[5] developed an ED specimen which produces Mode I behavior. The analysis was based on classical laminated plate theory and continuity of displacements, force resultants, and moment resultants between the cracked and uncracked regions of the plate were not satisfied. In addition, such an approach precludes any reasonable determination of the effect of specimen geometry on G_I.

Recently[6] Whitney developed a higher order laminated plate theory which includes transverse shear deformation and a thickness-stretch mode to analyze a Mode I ED specimen. The effect of specimen geometry on strain energy release rate was also investigated for 12 ply laminates of the class $[\theta/-\theta_2/\theta/90_2]_s$ and for the class $[0_3/90_3]_s$.

It is the purpose of the present work to develop a simple model for the analysis of Mixed-Mode ED specimens. Such a model provides closed-form estimates of G_I, G_{II} and G_{III} and hence allows one to establish appropriate failure criteria[7,8] for delamination.

Preliminary Remarks

Consider the ED specimen shown in Figure 1 subjected to a uniform strain $\varepsilon_x = \varepsilon$. Due to symmetry one quarter of the laminate is analyzed as shown in Figure 2. The response is only a function of Y and Z. The laminate is divided into sublaminates with thicknesses h_1 and h_o and local coordinate systems z_1, y_1 and z_o, y_o. The crack length is denoted by a. Sublaminates 1 and 2, and 0 and 3 represent the groups of plies above and below the interface along which delamination occurs, respectively.

In order to provide an accurate estimate of interlaminar stresses, a higher-order theory should be considered since classical laminated plate theory predicts zero interlaminar stresses. A shear deformation theory can be used for this purpose. This theory provides a good estimate for interlaminar shear stresses τ_{xz} and τ_{yz}. However, the interlaminar peel stress σ_{zz} is not accurate. The reason for that is the absence of thickness strain.

From symmetry, the transverse displacement w is zero at Z=0, hence the prescription of w at the middle plane Z=0 fixes w everywhere. In this case, the vertical shearing force resultant at both ends cannot be prescribed and the distribution of the peel stress will not be correct. Inspite of this simplification, reliable energy release rate components can be estimated based on interlaminar shear stresses. G_I is evaluated as $G_T - (G_{II}+G_{III})$, where the total energy release rate is denoted by G_T.

In the present formulation thickness strain is neglected and consequently considerable simplification in the analysis is achieved.

Another source of simplification in the present approach is due to the modeling of the structure as sublaminates---group of plies that are conveniently treated as laminated units. This approach can be applied with confidence if the characteristic length of the response is large compared to the individual sublaminate thickness.[9]

Overview of the Analytical Solution

In the following sections a step by step procedure is provided for the solution of the ED specimen. Intermediate results are also provided. The governing equations are derived in Appendix I. Expression for the interlaminar stresses, total energy release rate and energy release rate components are given in Equations (34), (40) and (42)-(43), respectively. The parameters associated with these equations are provided explicitly in terms of the stiffness coefficients in Appendix II.

A solution based on Classical Lamination Theory is given in Appendix III. This solution represents the behavior in the interior of the laminate. Application of the present analysis and comparison with a finite

element simulation for 63 test cases is presented under the section entitled Results and Discussion.

The reader interested in results and comparison can refer directly to the "Results and Discussion" section on page 28.

Analysis

Assume the following displacement field within each sublaminate:

$$\begin{aligned} u &= x\varepsilon + U(y) + z\beta_x(y) \\ v &= V(y) + z\beta_y(y) \\ w &= W(y) \end{aligned} \tag{1}$$

where u,v, and w denote displacements relative to the x, y, and z axes, respectively, and ε is a uniform axial strain. Coordinates y and z are local coordinates as shown in Figure 2. The present formulation recognizes shear deformation through the rotations β_x and β_y. The corresponding strains are

$$\begin{aligned} \varepsilon_{xx} &= \varepsilon \\ \varepsilon_{yy} &= V_{,y} + z\beta_{y,y} \\ \varepsilon_{zz} &= 0 \\ \gamma_{xy} &= U_{,y} + z\beta_{x,y} \\ \gamma_{xz} &= \beta_x \\ \gamma_{yz} &= \beta_y + W_{,y} \end{aligned} \tag{2}$$

The variables associated with sublaminates 0 through 3 will be written with subscripts 0 through 3, respectively.

From symmetry

$$w_o(y,-h_o/_2) = 0$$

or $$W_o = 0 \qquad (3)$$

From continuity of displacements at the interface between sublaminate (1) and (0)

$$u_o(y, h_o/2) = u_1(y,-h_1/2)$$
$$v_o(y, h_o/2) = u_1(y,-h_1/2)$$
$$w_o(y, h_o/2) = w_1(y,-h_1/2) \qquad (4)$$

Substitute from Equation (1) into (4) to get

$$U_o = U_1 - \frac{h_1}{2}\beta_{1x} - \frac{h_o}{2}\beta_{ox}$$

$$V_o = V_1 - \frac{h_1}{2}\beta_{1x} - \frac{h_o}{2}\beta_{ox}$$

$$W_1 = W_o = 0 \qquad (5)$$

Governing Equations

The governing equations for each sublaminate are derived in Appendix I using a virtual work approach. These equations are written below for convenience.

Constitutive Relationship

$$\begin{bmatrix} N_x \\ N_y \\ N_{xy} \\ M_x \\ M_y \\ M_{xy} \end{bmatrix} = \begin{bmatrix} A_{11} & A_{12} & A_{16} & B_{12} & B_{16} \\ A_{12} & A_{22} & A_{26} & B_{22} & B_{26} \\ A_{16} & A_{26} & A_{66} & B_{26} & B_{66} \\ B_{11} & B_{12} & B_{16} & D_{12} & D_{16} \\ B_{12} & B_{22} & B_{26} & D_{22} & D_{26} \\ B_{16} & B_{26} & B_{66} & D_{26} & D_{66} \end{bmatrix} \begin{bmatrix} \varepsilon \\ V_{,y} \\ U_{,y} \\ \beta_{y,y} \\ \beta_{x,y} \end{bmatrix}$$

$$\begin{bmatrix} Q_y \\ Q_x \end{bmatrix} = \begin{bmatrix} A_{44} & A_{45} \\ A_{45} & A_{55} \end{bmatrix} \begin{bmatrix} \beta_y + W_{,y} \\ \beta_x \end{bmatrix} \tag{6}$$

Equilibrium Equations

$$\begin{aligned} N_{xy,y} + n_x &= 0 \\ N_{y,y} + n_y &= 0 \\ Q_{y,y} + q &= 0 \\ M_{xy,y} - Q_x + m_x &= 0 \\ M_{y,y} - Q_y + m_y &= 0 \end{aligned} \tag{7}$$

where n_x, n_y, q, m_x and m_y are defined in Equation (I-9) of Appendix I.

The equilibrium equations can be written in terms of kinematic variables by substitution from Equation (6) into Equation (7). The result is

$$
\begin{bmatrix}
A_{66}L_{yy} & & & & \\
A_{26}L_{yy} & A_{22}L_{yy} & & \text{SYM} & \\
0 & 0 & -A_{44}L_{yy} & & \\
B_{66}L_{yy} & B_{26}L_{yy} & -A_{45}L_{y} & (D_{66}L_{yy} - A_{55}) & \\
B_{26}L_{yy} & B_{22}L_{yy} & -A_{44}L_{y} & (D_{26}L_{yy} - A_{45}) & (D_{22}L_{yy} - A_{44})
\end{bmatrix}
\begin{bmatrix} U \\ V \\ W \\ \beta_x \\ \beta_y \end{bmatrix}
= -
\begin{bmatrix} n_x \\ n_y \\ -q \\ m_x \\ m_y \end{bmatrix}
$$

$$
L_{yy} = d^2/dy^2
$$

$$
L_{y} = d/dy
$$

(8)

Solution Methodology

The above collection of equations are to be applied to individual plies of a laminate or to groups of plies... sublaminates. The solution steps are summarized in the following:

1. Divide the laminate into sublaminates according to geometry and loading condition. The sublaminate length is selected such that within the sublaminate the geometry and loading are continuous as is commonly done in engineering analysis of simple structures.
2. The displacements, resultant forces and moments, and interlaminar stresses in each sublaminate are governed by the equilibrium Equation(7), the constitutive relations (6) and the displacement distributions (1). Write these equations for each sublaminate in the analysis model.
3. Apply interlaminar continuity conditions and enforce traction or displacement conditions at the extreme upper and lower surfaces of the laminate.

4. Solve the system of coupled ordinary differential equations for the element variables.
5. Enforce the boundary conditions at constant values of y, the laminate sections, as well as continuity requirements between sublaminate ends in order to find the values of the arbitrary constants resulting from the solution in step 4.
6. Determine interlaminar stresses, resultant forces and moments displacement distribution and energy release rate.

Application to the ED Specimen

The ED configuration is divided into four sublaminates as shown in Figure 2. The response associated with sublaminates 1 and 0 is coupled through the continuity conditions at their common interface. Hence, the variables associated with both sublaminates are to be solved simulataneously. The situation is different with sublaminates 2 and 3 where the continuity conditions are relaxed due to the presence of the crack. Therefore, the variables associated with these sublaminates are not coupled.

The solution procedure for sublaminates 1 and 0--the uncracked portion of the laminate---is presented first, followed by the cracked portion represented by sublaminates 2 and 3.

Uncracked Region of the Laminate:

(i) Sublaminate 1

The upper surface of this sublaminate is stress free. Denote the shear and peel stress at the bottom surface by t_x, t_y and p, respectively, The transverse displacement W_1, is zero from Equation (5). Hence, the equilibrium equation in terms of the displacement variable takes the form

$$\begin{bmatrix} A_{66}{}^{1}L_{yy} & A_{26}{}^{1}L_{yy} & B_{66}{}^{1}L_{yy} & B_{26}{}^{1}L_{yy} \\ A_{26}{}^{1}L_{yy} & A_{22}{}^{1}L_{yy} & B_{26}{}^{1}L_{yy} & B_{22}{}^{1}L_{yy} \\ 0 & 0 & -A_{45}{}^{1}L_{y} & -A_{44}{}^{1}L_{y} \\ B_{66}{}^{1}L & B_{26}{}^{1}L_{yy} & (D_{66}{}^{1}L_{yy}-A_{55}{}^{1})(D_{26}{}^{1}L_{yy}-A_{45}{}^{1}) & \\ B_{26}{}^{1}L_{yy} & B_{22}{}^{1}L_{yy} & (D_{26}{}^{1}L_{yy}-A_{45}{}^{1})(D_{22}{}^{1}L_{yy}-A_{44}{}^{1}) & \end{bmatrix} \begin{bmatrix} U_1 \\ V_1 \\ \beta_{1x} \\ \beta_{1y} \end{bmatrix} = - \begin{bmatrix} -t_x \\ -t_y \\ p \\ \frac{h_1}{2} t_x \\ \frac{h_1}{2} t_y \end{bmatrix} \tag{9}$$

(ii) Sublaminate 0

From symmetry condition at the sublaminate bottom surface the shear stresses t_{1x} and t_{1y} are zero. From reciprocity of stresses at the interface between sublaminates 0 and 1, the interlaminar stresses at the upper surface of sublaminate 0 are t_x, t_y and p. Denote the peel stress at the sublaminate bottom surface by p_1. Hence the equlibrium equation takes the form

$$\begin{bmatrix} A_{66}{}^{o}L_{yy} & A_{26}{}^{o}L_{yy} & B_{66}{}^{o}L_{yy} & B_{26}{}^{o}L_{yy} \\ A_{26}{}^{o}L_{yy} & A_{22}{}^{o}L_{yy} & B_{26}{}^{o}L_{yy} & B_{22}{}^{o}L_{yy} \\ 0 & 0 & -A_{45}{}^{o}L_{y} & -A_{44}{}^{o}L_{y} \\ B_{66}{}^{o}L_{yy} & B_{26}{}^{o}L_{yy} & (D_{66}{}^{o}L_{yy}-A_{55}{}^{o}) & (D_{26}{}^{o}L_{yy}-A_{45}{}^{o}) \\ B_{26}{}^{o}L_{yy} & B_{22}{}^{o}L_{yy} & (D_{26}{}^{o}L_{yy}-A_{45}{}^{o}) & (D_{22}{}^{o}L_{yy}-A_{44}{}^{o}) \end{bmatrix} \begin{bmatrix} U_o \\ V_o \\ \beta_{ox} \\ \beta_{oy} \end{bmatrix} = - \begin{bmatrix} t_x \\ t_y \\ p_1-p \\ \frac{h_o}{2} t_x \\ \frac{h_o}{2} t_x \end{bmatrix} \tag{10}$$

Equations (9), (10) and (5) can be combined to yield the following form:

$$\begin{bmatrix} (F_{11}L_{yy}-A_{44}^{1}) & & \text{SYM} & \\ F_{21}L_{yy} & (F_{22}L_{yy}-A_{44}^{o}) & & \\ (F_{31}L_{yy}-A_{45}^{1}) & F_{32}L_{yy} & (F_{33}L_{yy}-A_{55}^{1}) & \\ F_{41}L_{yy} & (F_{42}L_{yy}-A_{45}^{o}) & F_{43}L_{yy} & (F_{44}L_{yy}-A_{55}^{o}) \end{bmatrix} \begin{bmatrix} \beta_{1y} \\ \beta_{oy} \\ \beta_{1x} \\ \beta_{ox} \end{bmatrix} = 0 \tag{11}$$

The parameters in Equation (11) are defined in Equation (II-1) of Appendix II.

Assume an exponential solution of the form

$$(\beta_{1y}, \beta_{oy}, \beta_{1x}, \beta_{ox}) = (\beta_{1y}^{*}, \beta_{oy}^{*}, \beta_{1x}^{*}, \beta_{ox}^{*})e^{sy} \tag{12}$$

Substitute from Equation (12) into Equation (11) to get the following characteristic equation

$$E_8 s^8 + E_6 s^6 + E_4 s^4 + E_2 s^2 + E_0 = 0 \tag{13}$$

Coefficients E_8 through E_0 are defined in Equation (II-5) of Appendix II. Parameter E_8 represents the determinant of the coefficients of L_{yy} in matrix equation (11) while E_0 is the determinant when L_{yy} is set to zero. Parameter E_0 depends solely on the stiffness coefficients A_{44}, A_{55} and A_{45} for both sublaminates while E_8 is predominantly influenced by the bending and coupling coefficients D_{ij} and B_{ij}. Hence its numerical value can be orders of magnitude smaller than the remaining coefficients. This fact results in the presence of a boundary zone in the response.

Typical values of a nondimensional form of the coefficients E_8 through E_0 is given in Table II for three laminates made of T300/5208 graphite/epoxy material. The nondimensional form of the coefficients is obtained by making the following substitution

$$\bar{s} = sb \tag{14}$$

Where b is the laminate semi-width. The arrows in the layups of Table II indicate the interfaces containing delaminations. The material properties and geometry appear in Table I.

The characteristic roots controlling the behavior are determined from Equation (13), which has a closed-form solution. However when A_{j6}, B_{j6}, D_{j6} (j = 1,2) and A_{45} are neglected, Equation (11) takes an uncoupled form and consequently the characteristic equation (13) can be factorized into two biquadratic equations. The stiffness coefficients A_{j6}, B_{j6} and D_{j6} represent coupling interaction while A_{45} depends predominantly on the shear modulii G_{31} and G_{23}. For a composite material where these shear modulii are approximately the same, A_{45} can be neglected.

The uncoupled form of the characteristic equation is

$$[(F_{11}F_{22}-F_{21}^2)s^4-(F_{11}A_{44}^{\,o} + F_{22}\,A_{44}^{\,1})s^2 + A_{44}^{\,1}A_{44}^{\,o}]$$

$$[(F_{33}F_{44}-F_{43}^2)s^4-(F_{33}A_{55}^{\,o} + F_{44}A_{55}^{\,1})s^2 + A_{55}^{\,o}A_{55}^{\,1}] = 0 \tag{15}$$

The first bracket in Equation (15) control V and β_y behavior while the second U and β_x. The absolute values of the roots in Equation (15) will be denoted by s_{y1}, s_{y2}, s_{x1} and s_{x2}. These can be regarded as a good approximation for the roots of the coupled equation (13). A comparison between the coupled and uncoupled roots for a typical laminate is provided in Table III. These roots are found to be real for the material system and layup used. The predictions of the uncoupled equation (15) are in good approximation with the coupled equation (13). Also, the larger characteristic roots s_{x1} and s_{y1} correspond to bending behavior while the smaller s_{x2} and s_{y2} control the membrane behavior. This is shown in the following section.

Membrane behavior can be modeled by setting

$$M_x = M_y = M_{xy} = 0 \tag{16}$$

in the equilibrium equations for sublaminates 1 and 0. The characteristic equation (13) reduces to

$$(F_{11m}s^2 - A_{44}^{-1})(F_{22m}s^2 - A_{55}^{-1}) = 0 \tag{17}$$

The membrane parameters F_{11m} and F_{22m} are defined in Equation (II-9) of Appendix II. They depend on A_{ij} and B_{ij} coefficients. The characteristic roots predicted by Equation (17) are included in Table III. By comparison with the roots of Equation (15), bending behavior is more localized than the membrane behavior as the characteristic roots controlling bending are larger. This fact is expected since Classical Lamination Theory (CLT), which predicts membrane-type behavior, prevails in the interior of the laminate.

Since the laminate width is large compared to its thickness and to the crack length, the response in sublaminates 1 and 0 is predominantly decaying from the crack tip and, therefore, only the roots with a negative sign will be considered in this solution.

Cracked Region of the Laminate:

Sublaminate 2

This sublaminate represents the upper group of plies in the cracked portion of the laminate. Since there is no restriction on the transverse displacement W, boundary conditions on Q can be specified.

The upper and lower surfaces in this sublaminate are stress-free and at y_1=-a there is a free edge. The equilibrium equation (7) reduces to

$$N_{xy_2} = N_{y_2} = Q_{y_2} = M_{y_2} = 0$$

$$M_{xy_{2,y}} - Q_{x_2} = 0 \qquad (18)$$

By substituting these conditions into the constitutive relations (6), to a single differential equation in terms of β_{2x} obtained.

$$(D_{66}{}^1 + B_{26}{}^1 Cd_{12} + B_{66}{}^1 Cd_{22} + D_{26}{}^1 Cd_{32})\, \beta_{2x,yy} - \left[A_{55}{}^1 - \frac{(A_{45}{}^1)^2}{A_{44}{}^1} \right] \beta_{2x} = 0 \qquad (19)$$

Parameters Cd_{12}, Cd_{22} and Cd_{32} are defined in Equation (II-10) of Appendix II. Solution of Equation (18) leads to

$$\beta_{2x} = H_1 e^{s_c y_1} + H_2 e^{-s_c y_1}$$

where $0 \leq y_1 \leq - a$

$$s_c = \left[\frac{A_{55}^{1} - (A_{45}^{1})^2/A_{44}^{1}}{(D_{66}^{1} + B_{26}^{1}Cd_{12} + B_{66}^{1}Cd_{22} + D_{26}^{1}Cd_{32})} \right]^{1/2} \tag{20}$$

Since the crack length 'a' can be small, positive as well as negative signs of the root s_c have been considered. The arbitrary constants H_1 and H_2 are determined from the boundary condition at

$$y_1 = -a \qquad M_{xy_2}(-a) = 0 \tag{21}$$

and continuity conditions at $y_1 = 0$ with sublaminate 1.

The displacements at the bottom surface of sublaminate 2 are

$$v_2(y_1, -h_1/2) = v_i(0) + (Cd_{11} - \frac{h_1}{2} Cd_{31})\, \varepsilon y_1 - (Cd_{12} - \frac{h_1}{2} Cd_{32})$$

$$[H_1 (1-e^{s_c y_1}) + H_2(1-e^{-s_c y_1})]$$

$$u_2(y_1-h_1/2) = u_i(0) + Cd_{21}\, \varepsilon y_1 - (Cd_{22} - \frac{h_1}{2}) [H_1(1-e^{s_c y_1}) + H_2(1-e^{-s_c y_1})] \tag{22}$$

where

$$v_i(0) = v_2(0, -h_1/2)$$

$$u_i(0) = u_2(0 - h_1/2)$$

The linear terms in y_1 in Equation (22) represent the displacement when $\beta_{2x} = 0$.

(ii) Sublaminate 3

The upper surface of this sublaminate is stress-free, while the interlaminar shear stresses on the lower surface are zero from symmetry conditions. Moreover, there is a free edge at $y_o = -a$. The equilibrium equation (7) reduces to

$$N_{xy_3} = N_{y_3} = 0$$

$$M_{xy_3,y} - Q_{x_3} = 0$$

$$M_{y_3,y} - Q_{y_3} = 0 \qquad (23)$$

By substituting these conditions into the constitutive relations (6), two coupled differential equations in β_{3y} and β_{3x} is obtained

$$\begin{bmatrix} J_{22}L_{yy} - A_{44}^{o} & J_{26}L_{yy} - A_{45}^{o} \\ J_{26}L_{yy} - A_{45}^{o} & J_{66}L_{yy} - A_{55}^{o} \end{bmatrix} \begin{bmatrix} \beta_{3y} \\ \beta_{3x} \end{bmatrix} = 0 \qquad (24)$$

Parameters J_{22} , J_{26} and J_{66} in Equation (24) are defined in Equation (II-12) of Appendix II.

Solve the differential equations for β_{3y} and β_{3x}.

$$\beta_{3y} = I_1 e^{ss_1 y_o} + I_2 e^{-ss_1 y_o} + I_3 e^{ss_2 y_o} + I_4 e^{-ss_2 y_o}$$

$$\beta_{3x} = \eta_1 (I_1 e^{ss_1 y_o} + I_2 e^{-ss_1 y_o}) + \eta_2 (I_3 e^{ss_2 y_o} + I_4 e^{-ss_2 y_o})$$

where $-a \leq y_o \leq 0$

$$\eta_j = - (J_{22} ss_j^2 - A_{44}^o) / (J_{26} ss_j^2 - A_{45}^o) \qquad (25)$$

The constants I_1 through I_4 are found from the boundary conditions at

$$y_o = -a \qquad M_{y_3}(-a) = M_{xy_3}(-a) = 0 \qquad (26)$$

and continuity conditions at $y_o = 0$ with sublaminate 0.

The roots ss_1 and ss_2 in Equation (25) are found by solving the characteristic equation resulting from equation (24).

The displacements at the upper surface of sublaminate 3 are given by

$$\begin{aligned} v_3(y_o, h_o/2) = {} & v_i(o) + wd_{11}\, \varepsilon y_o + (wd_{12} + \frac{h_o}{2} + \eta_1 wd_{13}) [I_1 (e^{ss_1 y_o} - 1) \\ & + I_2 (e^{-ss_1 y_o} - 1)] + (wd_{12} + \frac{h_o}{2} + \eta_2 wd_{13}) [I_3 (e^{ss_2 y_o} - 1) \\ & + I_4 (e^{-ss_2 y_o} - 1)] \end{aligned}$$

$$\begin{aligned} u_3(y_o, ho/2) = {} & u_i(o) + wd_{21}\, \varepsilon y_o + [wd_{22} + \eta_1 (wd_{23} + \frac{h_o}{2})] [I_1 (e^{ss_1 y_o} - 1) \\ & + I_2 (e^{-ss_1 y_o} - 1)] + [wd_{22} + \eta_2 (wd_{23} + \frac{h_o}{2})] [I_3 (e^{ss_2 y_o} - 1) \\ & + I_4 (e^{-ss_2 y_o} - 1)] \end{aligned} \qquad (27)$$

Parameters wd_{11}, wd_{12}, wd_{13}, wd_{21}, wd_{22}, and wd_{23} are defined in Equation (II-12) of Appendix II.

In order to determine the energy release rate components by the virtual crack-closure method[10], the relative displacements at the crack surface as well as the interlaminar stresses at the crack tip are needed. From Equations (22) and (27) the relative displacements are

$$\Delta v = v_3 (y_o, h_o/2) - v_2(y_1, -h_1/2)$$

$$= (wd_{11} - Cd_{11} + \frac{h_1}{2} Cd_{31})\, y\varepsilon + (wd_{12} + \frac{h_o}{2} + \eta_1 wd_{13})$$

$$[I_1 (e^{ss_1 y} - 1) + I_2 (e^{-ss_1 y} - 1)]$$

$$+ (wd_{12} + \frac{h_o}{2} + \eta_2 wd_{13}) [I_3(e^{ss_2 y} - 1) + I_4(e^{-ss_2 y} - 1)]$$

$$+ (Cd_{12} - \frac{h_1}{2} Cd_{32}) [H_1 (1 - e^{s_c y}) + H_2 (1 - e^{-s_c y})]$$

$$\Delta u = u_3(y_o, h_o/2) - u_2(y_1, -h_1/2)$$

$$= (wd_{21} - Cd_{21}) y\varepsilon + [wd_{22} + \eta_1 (wd_{23} + \frac{h_o}{2})] [I_1(e^{ss_1 y} - 1)$$

$$+ I_2 (e^{-ss_1 y} - 1)]$$

$$+ [wd_{22} + \eta_2 (wd_{23} + \frac{h_o}{2}) [I_3 (e^{ss_2 y} - 1) + I_4 (e^{-ss_2 y} - 1)]$$

$$+ (Cd_{22} - \frac{h_1}{2}) [H_1(1 - e^{s_c y}) + H_2 (1 - e^{-s_c y})]$$

$$-a \leq y \leq 0$$

(28)

The linear terms in Equation (28) represent the relative displacements when the shear deformations β_{2x}, β_{3x} and β_{3y} are neglected. The remaining terms are exponential, and their effect on the predictions are depicted in Figures 4 and 5, for two typical laminates. The dotted lines denoted by ΔU_L and ΔV_L in the figures correspond to the linear contribution, while the solid lines ΔU and ΔV include the exponential terms. The crack length 'a' in figures is 10 percent of the laminate semi-width and the applied strain is 1000 micro in/in. The simple linear distribution represents a good

approximation for the test cases considered. Due to the simplicity and accuracy of the linear displacement distribution, the energy release rate computations will be based on the linear displacement contribution only. A discussion of the effect of the exponential terms on the calculation of the total energy release rate will be provided later.

Interlaminar Stresses

Denote the absolute values of the roots in Equation (13) by s_j (j= 1,4). The response can be written in the form

$$\beta_{1y} = G_j e^{-s_j y}$$

$$\beta_{1x} = G_j \alpha_j e^{-s_j y}$$

$$\beta_{oy} = G_j \psi_j e^{-s_j y}$$

$$\beta_{ox} = G_j \gamma_j e^{-s_j y}$$

$$U_{1,y} = C_v - s_j v_j G_j e^{-s_j y}$$

$$V_{1,y} = C_u - s_j u_j G_j e^{-s_j y}$$

$$j = 1,4;\ o \leq y \leq b \qquad (29)$$

Summation over the range of index j is implied in Equation (29). Parameters α_j, ψ_j, γ_j, v_j, and u_j are defined in Equation (II-14) of Appendix II. The arbitrary constants of integration associated with the displacements are C_v and C_u.

Substitute from Equation (29) into the constitutive relationship for sublaminates 1 and 0 to get

$$\begin{bmatrix} N_{x_1} \\ N_{y_1} \\ N_{xy_1} \\ M_{y_1} \\ M_{xy_1} \end{bmatrix} = \begin{bmatrix} A_{11}^{1} & A_{12}^{1} & A_{16}^{1} \\ A_{12}^{1} & A_{22}^{1} & A_{26}^{1} \\ A_{16}^{1} & A_{26}^{1} & A_{66}^{1} \\ B_{12}^{1} & B_{22}^{1} & B_{26}^{1} \\ B_{16}^{1} & B_{26}^{1} & B_{66}^{1} \end{bmatrix} \begin{bmatrix} \varepsilon \\ C_v \\ C_u \end{bmatrix} - \begin{bmatrix} N_{x_{1j}} \\ N_{y_{1j}} \\ N_{xy_{1j}} \\ M_{y_{1j}} \\ M_{xy_{1j}} \end{bmatrix} s_j G_j e^{-s_j y}$$

$$\begin{bmatrix} Q_{y_1} \\ Q_{x_1} \end{bmatrix} = \begin{bmatrix} A_{44}^{1} & A_{45}^{1} \\ A_{45}^{1} & A_{55}^{1} \end{bmatrix} \begin{bmatrix} 1 \\ \alpha_j \end{bmatrix} G_j e^{-s_j y}$$

$$\begin{bmatrix} N_{x_o} \\ N_{y_o} \\ N_{xy_o} \\ M_{y_o} \\ M_{xy_o} \end{bmatrix} = \begin{bmatrix} A_{11}^{o} & A_{12}^{o} & A_{16}^{o} \\ A_{12}^{o} & A_{22}^{o} & A_{26}^{o} \\ A_{16}^{o} & A_{26}^{o} & A_{66}^{o} \\ B_{12}^{o} & B_{22}^{o} & B_{26}^{o} \\ B_{16}^{o} & B_{26}^{o} & B_{66}^{o} \end{bmatrix} \begin{bmatrix} \varepsilon \\ C_v \\ C_u \end{bmatrix} - \begin{bmatrix} N_{xoj} \\ -N_{y_{1j}} \\ -N_{xy_{1j}} \\ M_{yoj} \\ M_{xy_{oj}} \end{bmatrix} s_j G_j e^{-s_j y}$$

$$\begin{bmatrix} Q_{y_o} \\ Q_{xo} \end{bmatrix} = \begin{bmatrix} A_{44}^{o} & A_{45}^{o} \\ A_{45}^{o} & A_{55}^{o} \end{bmatrix} \begin{bmatrix} \psi_j \\ \gamma_j \end{bmatrix} G_j e^{-s_j y} \qquad (30)$$

The parameters associated with Equation (30) are defined in Equation (II-15) of Appendix II.

There are twelve arbitrary constants of integration namely: G_j (j= 1,4), C_v, C_u, H_1, H_2 and I_1 through I_4. These can be found from the boundary condition at the free edge of sublaminates 2 and 3 expressed in Equations (21) and (26) and from the continuity conditions between sublaminates 1 and 2, and 0 and 3 at y = 0. These are:

$$N_{y_1}(0) = N_{y_2}(0) = 0$$

$$N_{xy_1}(0) = N_{xy_2}(0) = 0$$

$$M_{y_1}(0) = M_{y_2}(0) = 0$$

$$N_{y_o}(0) = N_{y_3}(0) = 0$$

$$N_{xy_o}(0) = N_{xy_3}(0) = 0$$

$$M_{xy_2}(0) = M_{xy_1}(0)$$

$$M_{xy_o}(0) = M_{xy_3}(0)$$

$$M_{y_o}(0) = M_{y_3}(0)$$

$$\beta_{2x}(0) = \beta_{1x}(0)$$

$$\beta_{ox}(0) = \beta_{3x}(0)$$

$$\beta_{oy}(0) = \beta_{3y}(0) \qquad (31)$$

Boundary conditions on Q_y cannot be specified in sublaminates 1 and 0 as a result of neglecting the transverse normal strain in the assumed displacement function. Equations (21), (26) and (31) represent 14 boundary conditions for twelve constants. However, the last two continuity conditions at the interface between sublaminates 0 and 3 in Equation (31) lead to

$$A_{44}^{o}\,\beta_{oy}(0) + A_{45}^{o}\,\beta_{ox}(0) = A_{44}^{o}\,\beta_{3y}(0) + A_{45}^{o}\,\beta_{3x}(0)$$

that is,

$$Q_{y_o}(0) = Q_{y_3}(0) \tag{32}$$

which cannot be specified. Therefore, the conditions $\beta_{ox}(0) = \beta_{3x}(0)$ and $\beta_{oy}(0) = \beta_{3y}(0)$ cannot be prescribed for consistency.

Substitute for the resultant forces and moments in sublaminates 0 through 3 into the first nine equations in (31) and solve for the arbitrary constants. As C_v and C_u are easily obtained, their expressions are listed below for convenience.

$$C_v = (k_{26}\,k_{16} - k_{66}k_{12})\,\varepsilon/D$$
$$C_u = (k_{26}k_{12} - k_{22}\,k_{16})\,\varepsilon/D$$

where

$$k_{12} = A_{12}^{1} + A_{12}^{o}$$
$$k_{16} = A_{16}^{1} + A_{16}^{o} \tag{33}$$

Parameters k_{26}, k_{66}, k_{22} and D are defined in Equations (II-3) and (II-4).

The resultant axial forces and moments in Equation (30) consist of two parts: a constant term and an exponentially decaying term. In the interior of the laminate the second term is negligible and the response is controlled by the first term. Since CLT is retrieved in the interior of the laminate, the first term can be recognized as the CLT prediction. This is shown in Appendix III where a CLT solution is derived for the ED specimen. This solution is simple and can be derived on a ply-by-ply basis. Moreover, the sign of the resultant axial force N_y determines the sign of the interlaminar peel stress. A compressive peel stress tend to retard delamination at a given interface.

Interlaminar stresses at the interface between sublaminates 1 and 0 are found from equilibrium.

$$t_x = N_{xy_1},_y = N_{x_{1j}} \; s_j^2 \; G_j e^{-s_j y}$$

$$t_y = N_{y_1},_y = N_{y_1 j} \; s_j^2 \; G_j \; e^{-s_j y}$$

$$p = Q_{y_1},_y = -s_j (A_{44}{}^1 + A_{45}{}^1 \alpha_j) \; G_j e^{-s_j y} \tag{34}$$

The distribution of the peel stress p is not in equilibrium since the boundary condition on the shear force $Q_{y_1}(0)$ cannot be prescribed.

$$\int_0^b p dy = \int_0^b Q_{y_1},_y \, dy = Q_{y_1}(b) - Q_{y_1}(0) \tag{35}$$

$Q_{y_1}(b) \cong 0$ as Q_y is an exponentially decaying function, however $Q_{y_1}(0) \neq 0$.

A comparison of the interlaminar shear stress distribution t_y along the interface between sublaminates 1 and 0 appears in Figure 6 for three laminates. The applied uniform strain is 1000 micro in/in.

Energy Release Rate

The total energy release rate can be determined by considering the work done by external forces[5]. For a uniform applied strain $\varepsilon_x = \varepsilon$ throughout the laminate this can be written as

$$G_T = \frac{-\varepsilon}{2} \frac{dP}{da} \tag{36}$$

where P is the axial applied force and is given by

$$P = \int_o^{(b-a)} (N_{x_1} + N_{x_o})\, dy + \int_{-a}^{o} (N_{x_2} + N_{x_3})\, dy \tag{37}$$

The axial forces N_{x_1} and N_{x_o} in sublaminate 1 and 0 respectively are given in Equation (30) while the axial forces in sublaminate 2 and 3 are given by

$$N_{x2} = (A_{11}^{\,1} + A_{12}^{\,1}\, Cd_{11} + A_{16}^{\,1}\, Cd_{21} + B_{12}^{\,1}\, Cd_{31})\varepsilon + J_1 s_c (H_1 e^{s_c y} - H_2 e^{-s_c y})$$

$$N_{x3} = (A_{11}^{\,o} + A_{12}^{\,o}\, wd_{11} + A_{16}^{\,o}\, wd_{21})\varepsilon + (J_2 + \eta_1 J_3) ss_1 (I_1 e^{ss_1 y} - I_2 e^{-ss_1 y})$$

$$+ (J_2 + \eta_2 J_3)\, ss_2 (I_3 e^{ss_2 y} - I_4 e^{-ss_2 y}) \tag{38}$$

where

$$J_1 = B_{16}^{1} + A_{12}^{1} Cd_{12} + A_{16}^{1} Cd_{22} + B_{12}^{1} Cd_{32}$$

$$J_2 = B_{12}^{o} + A_{12}^{o} wd_{12} + A_{16}^{o} wd_{22}$$

$$J_3 = B_{16}^{o} + A_{13}^{o} wd_{13} + A_{16}^{o} wd_{23} \qquad (39)$$

Substitute from Equations (30) and (38) into Equation (36) and using Equation (37) to get

$$G_T = \frac{\varepsilon}{2} [K_{12} C_v + K_{16} C_u - (A_{12}^{1} Cd_{11} + A_{16}^{1} Cd_{21} + B_{12}^{1} Cd_{31})\varepsilon - (A_{12}^{o} wd_{11} + A_{16}^{o} wd_{21}) \varepsilon] + G_R \qquad (40)$$

where G_R is an exponential function of the crack length. For a crack length larger than a few ply thicknesses, the contribution of G_R is negligible. This situation is depicted in Figure 7 where a normalized total energy release rate for a typical laminate is plotted against the crack length divided by ply thickness. The laminate thickness is denoted by t in the figure and the ply thickness is h. In this case, G_T reaches the constant value predicted by the first term in Equation (40) for a value of crack length larger than four ply thickness. Also appearing in Figure 7 is a comparison with a finite element solution presented in Figure 6 of Reference 4.

The total energy release rate is a global parameter which does not depend strongly on the local details at the crack tip. This is the reason why relatively simple modeling approaches yield adequate predictions for the total energy release rate.

This finding checks the results of References 4 and 8 where simple closed-form expressions for G_T are in good agreement with predictions based on refined theories or on finite element simulation.

Energy Release Rate Components

Using the virtual crack-closure method G_{II} and G_{III} are given by

$$G_{II} = \lim_{\delta \to 0} \frac{1}{2\delta} \int_0^{\delta} t_y(\delta - r)\Delta v(r)dr$$

$$G_{III} = \lim_{\delta \to 0} \frac{1}{2\delta} \int_0^{\delta} t_x(\delta - r)\Delta u(r)dr \qquad (41)$$

where δ is a virtual crack step size. Unless a singularly exists in the stress field, Equation (41) yields the trivial result ($G_{II} = G_{III} = 0$) when the limit as δ tends to zero is determined.[9] Consequently, a sufficiently large finite step size is essential to get an answer when using models that do not exhibit singular behavior.

Subsitute from Equation (34) for the interlaminar stresses in term of force resultants into Equation (41) and use the linear terms in Equation (28) for the relative displacements to get

$$G_{II} = \frac{1}{2} \Theta_v \bar{F}_y$$

$$G_{III} = \frac{1}{2} \Theta_u \bar{F}_x$$

where

$$\Theta_v = wd_{11} - Cd_{11} + \frac{h_1}{2} Cd_{31}$$

$$\Theta_u = wd_{21} - Cd_{21}$$

$$\bar{F}_y = \frac{1}{\Delta} \int_0^{\Delta} N_{y_1} dy$$

$$\bar{F}_x = \frac{1}{\Delta} \int_0^{\Delta} N_{xy_1} dy \qquad (42)$$

The finite crack step size is denoted by Δ. The resultant forces N_{y1} and N_{xy1} exhibit a boundary layer behavior. This is shown in Figures 8 and 9 where the resultant force distributions are plotted along the laminate width. In the interior a constant value corresponding to the CLT prediction is reached.

The average resultant force values $\bar{F}_y$ and $\bar{F}_x$ depends on the selected value of the crack step Δ. Recommended ad hoc values as a percentage of the initial crack length have been suggested in the finite element representation of the crack-closure method.[11] However, within the boundary layer region N_{y1} and N_{xy1} have steep gradients and consequently a small variation in the selection of Δ leads to large variations in $\bar{F}_y$ and $\bar{F}_x$. Since N_{y1} and N_{xy1} distributions at the crack tip are controlled by the boundary layer decay length, the crack step size Δ should be selected based on the boundary layer length rather than a percentage of the initial crack length.

Mode I energy release rate is found from

$$G_I = G_T - (G_{II} + G_{III}) \qquad (43)$$

G_{II} and G_{III} are given in Equation (42) and G_T in Equation (40).

The energy release rate components predicted by this approach show a good correlation with finite element solutions when the crack step size Δ is selected as

$$\frac{\Delta}{b} = [\bar{s}_4 \ (\bar{s}_1 + \bar{s}_2 + \bar{s}_3)]^2 \qquad (44)$$

where $\bar{s}_j$ (j=1,4) are the characteristic roots in increasing magnitude nondimensionalized by the ply thickness h. The distinct roots s_j control the decay length associated with different physical variables. It has been found empirically that the combination above gives very good correlation with finite element simulations for over sixty cases that have been compared. Although the functional form is not simply identified with a boundary length it nevertheless contains the proper information.

For a general layup the crack size Δ is influenced by all four roots. However, for laminates where Mode III is negligible the crack step size is influenced by the characteristic roots s_2 and s_4 that control V and β_y behavior. For this situation, the following crack step size expression provides good correlation with the finite element solution:

$$\frac{\Delta}{b} = 2.6 \ (\bar{s}_4 \ \bar{s}_2)^2 \qquad (45)$$

Results and Discussion

An extensive comparison between the energy release rate components predicted by the present approach and a quasi 3-D finite element solution has been performed. The results appears in Tables IV through X and in Figures 10 through 28. The finite element results in Tables V through X

are related to the work of Reference 4 and were provided by the authors. The properties and geometry used appear in Table I. The applied uniform strain is one micro in/in.

In Table IV a comparison is provided for six laminates. The first three layups were reported in Reference 3. The G_{III} component in these layups are negligible. The remaining layups represent cases where G_I, G_{II} and G_{III} components are all finite.

The laminates presented in Tables V-X are rotated stacking sequences for two quasi-isotropic layups. The first is a $[0/90/\pm45]_s$ and the second is a $[45/90/-45/0]_s$. The results of the first laminate appear in Tables V-VII while in Tables VIII-X the results of the second laminate are provided. These laminates were used in Reference 4 to investigate delaminations around an open hole. The strain energy release rate distribution around the hole boundary, for delaminations growing in a prescribed interface, was calculated by assuming that each circumferencial portion acts as a straight edge subjected to an appropriate uniform circumferencial strain. Hence, at each circumferencial angle Θ the laminate reflects a new stacking sequence where the load is applied in the Θ-direction tangent to the hole. The angular position corresponding to each stacking sequence is provided in Tables V-X.

The results in Table V are plotted in Figures 10-12. In Figures 10 and 11 the percentages of G_{II} and G_{III} are plotted against the angular position, Θ, around a hole in the first laminate. The finite element results are shown in solid lines while the results of the present analysis appear in dotted lines. A comparison of G_T is shown in Figure 12. Similarly, the results in Table VI and VII are plotted in Figures 13-16 and

17-19, respectively. The results of the second laminate are provided in Tables VIII-X. The results in Table VIII are shown in Figures 20-22. Similarly the results of Tables IX and X are plotted in Figures 23-25 and 26-28. In Figures 22, 25 and 28 as well as in Tables VIII-X the values of G_T from the simple expression derived by O'Brien[4] are included for comparison. The plots in Figures 26-28 have been discontinued at $\theta = -45^o$ as compressive peel stress occurs at the 45/90 interface. The sign of the peel stress at a given interface can be determined from a simple membrane-type model. This is shown in Appendix III. Under compressive peel stress the crack surfaces tend to close and a special modeling approach should be used. One possible approach was proposed in Reference 9 in connection with a double cracked-lap-shear specimen tested under compression loading.

Conclusion

Interlaminar stresses and energy release rates are estimated for the ED test using a shear-type deformation theory and a sublaminate approach. The predictions are obtained in closed form and the parameters controlling the behavior are identified. The governing equations are derived using a virtual work approach. Due to the absence of transverse strain the interlaminar peel stress distribution is not in equilibrium. The interlaminar shear stresses, however, show reliable trends. The energy release rate components G_{II} and G_{III} are estimated based on the interlaminar shear stresses and relative displacements using the virtual crack closure method. The total energy release, G_T, is determined from the

rate of change of the work done by the external forces with crack length. Then G_I is obtained as the difference between G_T and $(G_{II} + G_{III})$.

An extensive comparison between the energy release rates predicted by the present approach and a quasi 3-D finite element solution for over sixty test cases, is performed. The agreement is good. The methodology outlined in this work is simple and the results are generated using a Hewlett Packard 9845B desktop computer.

ACKNOWLEDGEMENTS

The authors acknowledge the benefit of discussions and suggestions with Dr. Kevin O'Brien. The extensive comparison presented in this work for over sixty test cases was based on the finite element results of Dr. I.S. Raju.

Appendix I

Derivation of the Governing Equations

In this Appendix the governing equations for the sublaminate shown in Figure 3 are derived using the principle of virtual work.

Consider a sublaminate... a single ply or group of plies conveniently treated as laminated units of thickness h. The origin of a cartesian coordinate system is located within the central plane (x-y) with the z-axis being normal to this plane. The material of each ply is assumed to possess a plane of elastic symmetry parallel to xy as shown in Figure 3.

Stress and moment resultants,

$$(N_x,\ N_y,\ N_{xy},\ Q_x,\ Q_y) = \int_{-h/2}^{h/2} (\sigma_x,\ \sigma_y,\ \tau_{xz},\ \tau_{yz})\ dz$$

$$(M_x\ ,\ M_y,\ M_{xy}) = \int_{-h/2}^{h/2} (\sigma_x,\ \sigma_y,\ \tau_{xy})zdz \qquad \text{(I-1)}$$

Because of the existence of a plane of elastic symmetry, the constitutive relations are given by

$$\begin{bmatrix} \sigma_x \\ \sigma_y \\ \sigma_z \\ \tau_{xy} \end{bmatrix} = \begin{bmatrix} C_{11} & & & \\ C_{12} & C_{22} & \text{SYM} & \\ C_{13} & C_{23} & C_{33} & \\ C_{16} & C_{26} & C_{36} & C_{66} \end{bmatrix} \begin{bmatrix} \varepsilon_x \\ \varepsilon_y \\ \varepsilon_z \\ \gamma_{xy} \end{bmatrix}$$

$$\begin{bmatrix} \tau_{yz} \\ \tau_{xz} \end{bmatrix} = \begin{bmatrix} C_{44} & \text{SYM} \\ C_{45} & C_{55} \end{bmatrix} \begin{bmatrix} \gamma_{yz} \\ \gamma_{xz} \end{bmatrix} \qquad \text{(I-2)}$$

where C_{ij} are components of the anisotropic stiffness matrix and γ_{xy}, γ_{yz} and γ_{xz} are engineering shear strains

The displacements are assumed to be of the form

$$u \approx U(x,y) + z\beta_x(y)$$
$$v \approx V(y) + z\beta_y(y)$$
$$w \approx W(y) \qquad \text{(I-3)}$$

where u,v and w are the displacement components in the x, y and z directions, respectively. Equation (I-3) in conjunction with the strain-displacement relations of classical theory of elasticity leads to the following kinematic relations

$$\varepsilon_{xx} = U_{,x}$$
$$\varepsilon_{yy} = V_{,y} + z\beta_{y,y}$$
$$\varepsilon_{zz} = 0$$
$$\gamma_{xy} = V_{,y} + z\beta_{x,y}$$
$$\gamma_{xz} = \beta_x$$
$$\gamma_{yz} = \beta_y + W_{,y} \qquad \text{(I-4)}$$

Substitute Equation (I-4) into Equation (I-2) and put the results into Equation (I-1). This yields the following constitutive relations:

$$\begin{bmatrix} N_x \\ N_y \\ N_{xy} \\ M_x \\ M_y \\ M_{xy} \end{bmatrix} = \begin{bmatrix} A_{11} & A_{12} & A_{16} & B_{11} & B_{12} & B_{16} \\ A_{12} & A_{22} & A_{26} & B_{12} & B_{22} & B_{26} \\ A_{16} & A_{26} & A_{66} & B_{16} & B_{26} & B_{66} \\ B_{11} & B_{12} & B_{16} & D_{11} & D_{12} & D_{16} \\ B_{12} & B_{22} & B_{26} & D_{12} & D_{22} & D_{26} \\ B_{16} & B_{26} & B_{66} & D_{16} & D_{26} & D_{66} \end{bmatrix} \begin{bmatrix} U,_x \\ V,_y \\ U,_y \\ 0 \\ \beta_{y,y} \\ \beta_{x,y} \end{bmatrix}$$

$$\begin{bmatrix} Q_y \\ Q_x \end{bmatrix} = \begin{bmatrix} A_{44} & A_{45} \\ A_{45} & A_{55} \end{bmatrix} \begin{bmatrix} \beta_y + W,_y \\ \beta_x \end{bmatrix}$$

where

$$(A_{ij}; B_{ij}, D_{ij}) = \int_{-h/2}^{h/2} C_{ij} (1, z, z^2) dz \qquad \text{(I-5)}$$

The usual coupling between bending and extensional modes for a laminate of arbitrary construction occurs in Equation (I-5) through the stiffness terms B_{ij}.

The variation of the strain energy due to virtual displacements δu, δv and δw is

$$\delta \bar{V} = \int_V (\sigma_x \delta\varepsilon_x + \sigma_y \delta\varepsilon_y + \sigma_z \delta\varepsilon_z + \tau_{xy} \delta\gamma_{xy} + \tau_{yz} \delta\gamma_{yz} + \tau_{xz} \delta\gamma_{xz}) dV \qquad \text{(I-6)}$$

where $\delta\varepsilon_x$, $\delta\varepsilon_y$, $\delta\varepsilon_z$, $\delta\gamma_{xy}$, $\delta\gamma_{yz}$ and $\delta\gamma_{xz}$ are the strains associated with the virtual displacements. Substitute from Equation (I-3) and integrate through the thickness using Equation (I-1) to get

$$\delta\bar{U} = \int_A [N_x\, \delta U,_x + N_y \delta V,_y + N_{xy}\, \delta U,_y + Q_x\, \delta\beta_x + Q_y\, (\delta\beta_y + \delta W,_y) + M_x \delta\beta_{x,x} + M_y\, \delta\beta_{y,y} + M_{xy}\, \delta\beta_{x,y}]\, dA \qquad (I\text{-}7)$$

The variation of the work done by the external forces and by the surface fractions is

$$\delta\bar{W} = \int_A (n_x\, \delta U + n_y\, \delta V + q\delta W + m_x \delta\beta_x + m_y\, \delta\beta_y)\, dA + \int_S (\bar{N}_n\, \delta\bar{U}_n + \bar{N}_{ns}\, \delta\bar{U}_s + \bar{M}_n\, \delta\bar{\beta}_n + \bar{M}_{ns}\delta\bar{\beta}_s)ds \qquad (I\text{-}8)$$

where a bar denotes values on the boundary, n and s are coordinates normal and tangential to the edge, and

$$\begin{aligned} n_x &= t_{2x} - t_{1x} \\ n_y &= t_{2y} - t_{1y} \\ q &= p_2 - p_1 \\ m_x &= \frac{h}{2}\,(t_{2x} + t_{1x}) \\ m_y &= \frac{h}{2}\,(t_{2y} + t_{1y}) \end{aligned} \qquad (I\text{-}9)$$

where n_x and n_y can be regarded as effective distributed axial forces, m_x and m_y effective distributed moments and q an effective lateral pressure.

From the principle of virtual work the equations of equilibrium and boundary conditions are determined from the Euler equations and boundary conditions of the variational equation.

$$\delta\bar{V} = \delta\bar{W} \tag{I-10}$$

Substitution of Equations (I-7) and (I-8) into Equation (I-10) leads the following equations of equilibrium:

$$\begin{aligned} N_{x,x} + N_{xy,y} + n_x &= 0 \\ N_{xy,x} + N_{y,y} + n_y &= 0 \\ Q_{x,x} + Q_{y,y} + q &= 0 \\ M_{x,x} + M_{xy,y} - Q_x + m_x &= 0 \\ M_{xy,x} + M_{y,y} - Q_y + m_y &= 0 \end{aligned} \tag{I-11}$$

and one member of the following five products must be prescribed on the sublaminate edges

$$N_n\, U_n,\ N_{ns} U_s,\ M_n \beta_n,\ M_{ns}\, \beta_s \text{ and } Q_n\, W \tag{I-12}$$

For the ED specimen under uniform extension, U(x,y) in Equation (I-3) is given by

$$U(x,y) = x\varepsilon + U^*(y) \tag{I-13}$$

and the response is a function of y and z coordinates only. For this case the equilibrium equations (I-11) take the form

$$N_{xy,y} + n_x = 0$$

$$N_{y,y} + n_y = 0$$

$$Q_{y,y} + q = 0$$

$$M_{xy,y} - Q_x + m_x = 0$$

$$M_{y,y} - Q_y + m_y = 0$$

(I-14)

Substitution of the constitutive relations in Equation (I-5) into Equation

$$\begin{bmatrix} A_{66}L_{yy} & & & & \\ A_{26}L_{yy} & A_{22}L_{yy} & & \text{SYM} & \\ 0 & 0 & -A_{44}L_{yy} & & \\ B_{66}L_{yy} & B_{26}L_{yy} & -A_{45}L_y & (D_{66}L_{yy} - A_{55}) & \\ B_{26}L_{yy} & B_{22}L_{yy} & -A_{44}L_y & (D_{26}L_{yy} - A_{45}) & (D_{22}L_{yy} - A_{44}) \end{bmatrix} \begin{bmatrix} U^* \\ V \\ W \\ \beta_x \\ \beta_y \end{bmatrix} = - \begin{bmatrix} n_x \\ n_y \\ -q \\ m_x \\ m_y \end{bmatrix}$$

(I-15)

where the operators

$$L_{yy} = d^2/dy^2$$

$$L_y = d/dy \qquad \text{(I-16)}$$

and for the boundary conditions at y = constant prescribe

$$N_{xy} \text{ or } U^*,\ N_y \text{ or } V,\ Q_y \text{ or } W,\ M_y \text{ or } \beta_y \text{ and } M_{xy} \text{ or } \beta_x \qquad \text{(I-17)}$$

Appendix II

Definition of Parameters

In this appendix the parameters in Equations (11) - (30) are defined in terms of the sublaminates thickness and A_{ij}, B_{ij} and D_{ij} coefficients.

Sublaminates 1 and 0:

The F_{ij} parameters (i=1-3, j=1-4) in Equation (11) are defined as

$$F_{11} = D_{22}^{1} + \frac{h_1}{2} B_{22}^{1} + h_{22} v_{11} + h_{26} u_{11}$$

$$F_{21} = h_{22} v_{12} - h_{26} u_{12}$$

$$F_{31} = D_{26}^{1} + \frac{h_1}{2} B_{26}^{1} + h_{22} v_{13} + h_{26} u_{13}$$

$$F_{41} = h_{22} v_{14} + h_{26} u_{14}$$

$$F_{22} = D_{22}^{o} - \frac{h_o}{2} B_{22}^{o} + C_{22} v_{12} + C_{26} u_{12}$$

$$F_{32} = h_{26} v_{12} + h_{66} u_{12}$$

$$F_{43} = h_{26} v_{14} + h_{66} u_{14}$$

$$F_{33} = D_{66}^{1} + \frac{h_1}{2} B_{66}^{1} + h_{26} v_{13} h_{66} u_{13}$$

$$F_{42} = D_{26}^{o} - \frac{h_o}{2} B_{26}^{o} + C_{22} v_{14} + C_{26} u_{14}$$

$$F_{44} = D_{66}^{o} - \frac{h_o}{2} B_{66}^{o} + C_{26} v_{14} + C_{66} u_{14} \qquad \text{(II-1)}$$

Parameters u_{1i} and v_{1i} (i= 1-4) in Equation (II-1) relate the displacements U_1 and V_1 to the rotations through the following equation

$$\begin{bmatrix} V_{1,yy} \\ U_{1,yy} \end{bmatrix} = \begin{bmatrix} v_{11}L_{yy} & v_{12}L_{yy} & v_{13}L_{yy} & v_{14}L_{yy} \\ u_{11}L_{yy} & u_{12}L_{yy} & u_{13}L_{yy} & u_{14}L_{yy} \end{bmatrix} \begin{bmatrix} \beta_{1y} \\ \beta_{oy} \\ \beta_{1x} \\ \beta_{ox} \end{bmatrix} \qquad \text{(II-2)}$$

where

$$v_{11} = (K_{26}\, h_{26} - K_{66}\, h_{22})/D + h_1/2$$

$$v_{12} = (K_{26}C_{26} - K_{66}\, C_{22})/\, D + h_o/2$$

$$v_{13} = (K_{26}\, h_{66} - K_{66}\, h_{26})/D$$

$$v_{14} = (K_{26}\, C_{66} - K_{66}\, C_{26})/D$$

$$u_{11} = (K_{26}h_{22} - K_{22}h_{26})/D$$

$$u_{12} = (K_{26}C_{22} - K_{22}C_{26})/D$$

$$u_{13} = (K_{26}h_{26} - K_{22}h_{66})/D + h_1/2$$

$$u_{14} = (K_{26}C_{26} - K_{22}C_{66})/D + h_o/2$$

$$D = K_{22}K_{66} - K_{26}^2 \qquad \text{(II-3)}$$

and

$$h_{22} = B_{22}^{1} + \frac{h_1}{2} A_{22}^{1}$$

$$h_{26} = B_{26}^{1} + \frac{h_1}{2} A_{26}^{1}$$

$$h_{66} = B_{66}^{1} + \frac{h_1}{2} A_{66}^{1}$$

$$C_{22} = B_{22}^{o} + \frac{h_o}{2} A_{22}^{1}$$

$$C_{26} = B_{26}^{o} + \frac{h_o}{2} A_{26}^{1}$$

$$C_{66} = B_{66}^{o} + \frac{h_o}{2} A_{66}^{1}$$

$$K_{22} = A_{22}^{1} + A_{22}^{o}$$

$$K_{26} = A_{26}^{1} + A_{26}^{o}$$

$$K_{66} = A_{66}^{1} + A_{66}^{1} \qquad \text{(II-4)}$$

The coefficients E_8 through E_0 in Equation (13) are defined as

$$E_8 = F_{11}W_1 - F_{31}X_1 + F_{21}Y_1 - F_{41}Z_1$$

$$E_6 = F_{11}W_2 - A_{44}^{1}W_1 - F_{31}X_2 + A_{45}^{1}X_1 + F_{21}Y_2 - F_{41}Z_2$$

$$E_4 = [A_{44}^{o}A_{55}^{o} - (A_{45}^{o})^2](F_{11}F_{33} - F_{31}^2) + (F_{22}A_{55}^{o} + F_{44}A_{44}^{o} - 2F_{42}A_{45}^{o})(F_{11}A_{55}^{1} - F_{31}A_{45}^{1}) - A_{44}^{1}W_2 + A_{45}^{1}X_2 + F_{21}Y_3 - F_{41}Z_3$$

$$E_2 = -[A_{44}^{o}A_{55}^{o} - (A_{45}^{o})^2][F_{11}A_{55}^{1} + F_{33}A_{44}^{1} - 2F_{31}A_{45}^{1}] - [A_{44}^{1}A_{55}^{1} - (A_{45}^{1})^2](F_{22}A_{55}^{o} + F_{44}A_{44}^{o} - 2F_{42}A_{45}^{o})$$

$$E_0 = [A_{44}^{o}A_{55}^{o} - (A_{45}^{o})^2][A_{44}^{1}A_{55}^{1} - (A_{45}^{1})^2]$$

where

$$W_1 = F_{33}(F_{22}F_{44} - F_{42}^2) - F_{32}^2 F_{44} + 2F_{43}F_{42} - F_{43}^2 F_{22}$$

$$W_2 = F_{33}(F_{22}A_{55}^o + F_{44}A_{44}^o - 2F_{42}A_{45}^o) - A_{55}^1(F_{22}F_{44} - F_{42}^2)$$

$$+ F_{32}^2 A_{55}^o - 2F_{43}F_{32}A_{45}^o + F_{43}^2 A_{44}^o$$

$$X_1 = F_{31}(F_{22}F_{44} - F_{42}^2) - F_{32}(F_{21}F_{44} - F_{41}F_{42}) + F_{43}(F_{21}F_{42} - F_{41}F_{22})$$

$$X_2 = -F_{31}(F_{22}A_{55}^o + F_{44}A_{44}^o - 2F_{42}A_{45}^o) - A_{45}^1(F_{22}F_{44} - F_{42}^2)$$

$$+ F_{32}(F_{21}A_{55}^o - F_{41}A_{45}^o) - F_{43}(F_{21}A_{45}^o - F_{41}A_{44}^o)$$

$$Y_1 = F_{31}(F_{32}F_{44} - F_{43}F_{42}) - F_{33}(F_{21}F_{44} - F_{41}F_{42}) + F_{43}(F_{21}F_{43} - F_{41}F_{32})$$

$$Y_2 = -A_{45}^1(F_{32}F_{44} - F_{43}F_{42}) - F_{31}(F_{32}A_{55}^o - F_{43}A_{45}^o)$$

$$+ A_{55}^1(F_{21}F_{44} - F_{41}F_{42}) + F_{33}(F_{21}A_{55}^o - F_{41}A_{45}^o)$$

$$Y_3 = A_{45}^1(F_{32}A_{55}^o - F_{43}A_{45}^o) - A_{55}^1(F_{21}A_{55}^o - F_{41}A_{45}^o)$$

$$Z_1 = F_{31}(F_{32}F_{42} - F_{43}F_{22}) - F_{33}(F_{21}F_{42} - F_{41}F_{22}) + F_{32}(F_{21}F_{43} - F_{41}F_{32})$$

$$Z_2 = F_{31}(F_{43}A_{44}^o - F_{32}A_{45}^o) - A_{45}^1(F_{32}F_{42} - F_{43}F_{22}) + A_{55}^1(F_{21}F_{42} - F_{41}F_{22})$$

$$- F_{33}(F_{41}A_{44}^o - F_{21}A_{45}^o)$$

$$Z_3 = -A_{45}^1(F_{43}A_{44}^o - F_{32}A_{45}^o) + A_{55}^1(F_{41}A_{44}^o - F_{21}A_{45}^o)$$

(II-5)

when the coefficients A_{j6}, B_{j6}, D_{j6} (j=1,2) and A_{45} are neglected

we have

$$v_{13} = v_{14} = u_{11} = u_{12} = 0$$

and

$$F_{31} = F_{41} = F_{32} = F_{42} = 0 \qquad \text{(II-6)}$$

for this case Equation (II-2) is

$$\begin{bmatrix} V_{1,yy} \\ U_{1,yy} \end{bmatrix} = \begin{bmatrix} v_{11}L_{yy} & v_{12}L_{yy} & 0 & 0 \\ 0 & 0 & u_{13}L_{yy} & u_{14}L_{yy} \end{bmatrix} \begin{bmatrix} \beta_{1y} \\ \beta_{oy} \\ \beta_{1x} \\ \beta_{ox} \end{bmatrix}$$

(II-7)

and Equation (11) takes the uncoupled form

$$\begin{bmatrix} (F_{11}L_{yy} - A_{44}^{1}) & & & \text{SYM} \\ F_{21}L_{yy} & (F_{22}L_{yy} - A_{44}^{o}) & & \\ 0 & 0 & (F_{33}L_{yy} - A_{55}^{1}) & \\ 0 & 0 & F_{43}L_{yy} & (F_{44}L_{yy} - A_{55}^{o}) \end{bmatrix} \begin{bmatrix} \beta_{1y} \\ \beta_{oy} \\ \beta_{1x} \\ \beta_{ox} \end{bmatrix} = 0$$

(II-8)

By neglecting bending effects in sublaminates 1 and 0, the rotations β_{oy} and β_{ox} can be expressed in terms of β_{1y} and β_{1x} and the characteristic equation reduces to

$$(F_{11m}s^2 - A_{44}^{1})\,(F_{22m}s^2 - A_{55}^{1}) = 0$$

where

$$F_{11m} = \frac{h_1}{2}\left[A_{22}^{1}\left(v_{11} + v_{12}\,\frac{h_o}{h_1}\,\frac{A_{44}^{1}}{A_{44}^{o}}\right) + B_{22}^{1}\right]$$

$$F_{22m} = \frac{h_2}{2}\left[A_{66}^{1}\left(u_{13} + u_{14}\,\frac{h_o}{h_1}\,\frac{A_{55}^{1}}{A_{55}^{o}}\right) + B_{66}^{1}\right] \qquad \text{(II-9)}$$

Parameters F_{11m} and F_{22m} represent a membrane behavior and therefore do not depend on the bending coefficients D_{ij}.

Sublaminate 2:

The elements of the matrix Cd in Equation (19) are defined as

$$[Cd]_{3x2} = -\begin{bmatrix} A_{22}^{1} & & \text{SYM} \\ A_{26}^{1} & A_{66}^{1} & \\ B_{22}^{1} & B_{26}^{1} & D_{22}^{1} \end{bmatrix}^{-1} \begin{bmatrix} A_{12}^{1} & B_{26}^{1} \\ A_{16}^{1} & B_{66}^{1} \\ B_{12}^{1} & D_{26}^{1} \end{bmatrix} \qquad \text{(II-10)}$$

Displacements U_2 and V_2 and rotation β_{2y} in sublaminate 2 are related to the applied uniform strain ε and the rotation β_{2x} through the matrix Cd by

$$\begin{bmatrix} V_{2,y} \\ U_{2,y} \\ \beta_{2y,y} \end{bmatrix} = [Cd] \begin{bmatrix} \varepsilon \\ \beta_{2x,y} \end{bmatrix} \qquad \text{(II-11)}$$

Sublaminate 3:

Parameters J_{22}, J_{26} and J_{66} in Equation (24) are defined by

$$J_{22} = D_{22}^{o} + B_{22}^{o}\ wd_{12} + B_{26}^{o}\ wd_{22}$$

$$J_{26} = D_{26}^{o} + B_{22}^{o}\ wd_{13} + B_{26}^{o}\ wd_{23}$$

$$J_{66} = D_{66}^{o} + B_{26}^{o}\ wd_{13} + B_{66}^{o}\ wd_{23}$$

where

$$[wd]_{2x3} = - \begin{bmatrix} A_{22}^{o} & A_{26}^{o} \\ A_{26}^{o} & A_{66}^{o} \end{bmatrix}^{-1} \begin{bmatrix} A_{12}^{o} & B_{22}^{o} & B_{26}^{o} \\ A_{16}^{o} & B_{26}^{o} & B_{66}^{o} \end{bmatrix} \qquad \text{(II-12)}$$

Displacements U_3 and V_3 in sublaminate 3 are related to the applied uniform strain ε and the rotations β_{3x} and β_{3y} through the matrix wd by

$$\begin{bmatrix} V_3 \\ U_3 \end{bmatrix} = [wd] \begin{bmatrix} \varepsilon \\ \beta_{3y,y} \\ \beta_{3x,y} \end{bmatrix} \qquad \text{(II-13)}$$

Interlaminar Stresses:

Parameters α_j, ψ_j and γ_j in Equation (29) are defined as

$$\begin{bmatrix} \alpha_j \\ \psi_j \\ \gamma_j \end{bmatrix} = - \begin{bmatrix} (F_{31}s_j^2 - A_{45}^1) & F_{21}^2 s_j & F_{41}s_j^2 \\ (F_{33}s_j^2 - A_{55}^1) & F_{32}s_j^2 & F_{43}s_j^2 \\ (F_{32}s_j^2 & (F_{22}\, s_j^2 - A_{44}^o) & (F_{42}\, s_j^2 - A_{45}^o) \end{bmatrix}^{-1} \begin{bmatrix} (F_{11}s_j^2 - A_{44}^1) \\ (F_{31}s_j^2 - A_{45}^1) \\ F_{21}s_j^2 \end{bmatrix}$$

$$v_j = v_{11} + \alpha_j\, v_{13} + \psi_j v_{12} + \gamma_j v_{14}$$

$$u_j = u_{11} + \alpha_j\, u_{13} + \psi_j u_{12} + \gamma_j u_{14} \qquad \text{(II-14)}$$

The parameters associated with the resultant force and moment distributions in sublaminates 1 and 0, Equation (30) are given by

$$\begin{bmatrix} N_{x1j} \\ N_{y1j} \\ N_{xy1j} \\ M_{y1j} \\ M_{xy1j} \end{bmatrix} = \begin{bmatrix} A_{12}^1 & A_{16}^1 & B_{12}^1 & B_{16}^1 \\ A_{22}^1 & A_{26}^1 & B_{22}^1 & B_{26}^1 \\ A_{26}^1 & A_{66}^1 & B_{26}^1 & B_{66}^1 \\ B_{22}^1 & B_{26}^1 & D_{22}^1 & D_{26}^1 \\ B_{26}^1 & B_{66}^1 & D_{26}^1 & D_{66}^1 \end{bmatrix} \begin{bmatrix} v_j \\ u_j \\ 1 \\ \alpha_j \end{bmatrix}$$

$$\begin{bmatrix} N_{xoj} \\ N_{yoj} \\ N_{xyoj} \\ M_{yoj} \\ M_{xyoj} \end{bmatrix} = \begin{bmatrix} A_{12}^{o} & A_{16}^{o} & (B_{12}^{o} - \frac{h_o}{2} A_{12}^{o}) & (B_{16}^{o} - \frac{h_o}{2} A_{16}^{o}) - \frac{h_1}{2} A_{12}^{o} - \frac{h_1}{2} A_{16}^{o} \\ A_{22}^{o} & A_{26}^{o} & (B_{22}^{o} - \frac{h_o}{2} A_{22}^{o}) & (B_{26}^{o} - \frac{h_o}{2} A_{26}^{o}) - \frac{h_1}{2} A_{22}^{o} - \frac{h_1}{2} A_{26}^{o} \\ A_{26}^{o} & A_{66}^{o} & (B_{26}^{o} - \frac{h_o}{2} A_{26}^{o}) & (B_{66}^{o} - \frac{h_o}{2} A_{66}^{o}) - \frac{h_1}{2} A_{26}^{o} - \frac{h_1}{2} A_{66}^{o} \\ B_{22}^{o} & B_{26}^{o} & (D_{22}^{o} - \frac{h_o}{2} B_{26}^{o}) & (D_{26}^{o} - \frac{h_o}{2} B_{26}^{o}) - \frac{h_1}{2} B_{26}^{o} - \frac{h_1}{2} B_{26}^{o} \\ B_{26}^{o} & B_{66}^{o} & (D_{26}^{o} - \frac{h_o}{2} B_{22}^{o}) & (D_{66}^{o} - \frac{h_o}{2} B_{66}^{o}) - \frac{h_1}{2} B_{26}^{o} - \frac{h_1}{2} B_{66}^{o} \end{bmatrix} \begin{bmatrix} v_j \\ u_j \\ \psi_j \\ \gamma_j \\ 1 \\ \alpha_j \end{bmatrix}$$

(II-15)

Appendix III

Classical Lamination Theory (CLT) Solution

In the interior of the laminate CLT prevails that is, a membrane solution controls the behavior. The resultant forces N_y and N_{xy} are easily determined. In the following a ply-by-ply model is constructed.

The constitutive relationship for each ply for a membrance behavior is given by

$$\begin{bmatrix} N_x \\ N_y \\ N_{xy} \end{bmatrix}^k = \begin{bmatrix} A_{11} & A_{12} & A_{16} \\ A_{12} & A_{22} & A_{26} \\ A_{16} & A_{26} & A_{66} \end{bmatrix}^k \begin{bmatrix} \varepsilon \\ \varepsilon_y \\ \gamma_x \end{bmatrix}^k \qquad \text{(III-1)}$$

Superscript k denotes the kth ply. According to the present formulation

$$\varepsilon_y = V(y),_y$$

$$\gamma_x = U(y),_y \qquad \text{(III-2)}$$

Since ε_y and γ_x are functions of y only, therefore, from continuity of displacements at the interfaces between the kth and (k+1)th plies we have

$$u^k(y, \frac{h}{2}) = u^{k+1}(y, \frac{-h^{k+1}}{2})$$

$$v^k(y, \frac{h^k}{2}) = v^{k+1}(y, \frac{-h^{k+1}}{2}) \qquad \text{(III-3)}$$

Substitute for the displacements from Equation (1) into Equation (III-3) and differentiate w.r.t. y to get

$$\varepsilon_y^{\,k} = \varepsilon_y^{\,k+1} = \varepsilon_y$$

$$\gamma_x^{\,k} = \gamma_x^{\,k+1} = \gamma_x \qquad \text{(III-4)}$$

From symmetry, consider one quarter of the laminate. From equilibrium of forces get

$$\sum_{k=1}^{N} N_y^{\,k} = \sum_{k=1}^{N} N_{xy}^{\,k} = 0 \qquad \text{(III-5)}$$

Substitute from Equation (III-1) into (III-5) to get

$$s_{22}\,\varepsilon_y + s_{26}\,\gamma_x + s_{12}\,\varepsilon = 0$$

$$s_{26}\,\varepsilon_y + s_{66}\,\gamma_x + s_{16}\,\varepsilon = 0$$

where

$$s_{\ell m} = \sum_{k=1}^{N} A_{\ell m}^{\,k} \qquad \ell = 1,2 \quad m = 2 \text{ and } 6 \qquad \text{(III-6)}$$

Solving for ε_y and γ_x from Equation (III-6) to get

$$\varepsilon_y = (s_{26}s_{16} - s_{66}s_{12})\varepsilon/s$$

$$\gamma_x = (s_{26}s_{12} - s_{22}s_{16})\varepsilon/s \qquad \text{(III-7)}$$

$$s = s_{22}\,s_{66} - (s_{26})^2$$

Substituting from Equation (III-7) into Equation (III-1) to get

$$N_y^k = (A_{12}^k \varepsilon + A_{22}^k \varepsilon_y + A_{26}^k \gamma_x)$$

$$N_{xy}^k = (A_{16}^k \varepsilon + A_{26}^k \varepsilon_y + A_{66}^k \gamma_x) \qquad \text{(III-8)}$$

By comparing the expressions for C_v and C_u in Equation (33) with Equation (III-7), we find that for sublaminates 1 and 0

$$C_v = \varepsilon_y$$

and

$$C_u = \gamma_x \qquad \text{(III-9)}$$

Therefore the first term in Equation (30) for N_x, N_y and N_{xy} in sublaminate 1 and 0 is the CLT prediction.

From equilibrium considerations the sign of the resultant axial force N_y^k in each ply determines the sign of the interlaminar peel stress. This is illustrated for a $[0_{\uparrow}/45/90/-45]_s$ with a delamination at the 0/45 interface. With reference to Figure 26, this layup corresponds to a $[45_{\uparrow}/90/-45/0]_s$ laminate rotated at an angle $\theta = -45$.

For the properties shown in Table I and using Equations (III-7) and (III-8) the resultant forces N_y and N_{xy} in each ply can be determined. These are shown in Table XI.

Consider the free body diagram of the top ply shown in Figure 29. From equilibrium of forces in the vertical direction the peel stress distribution should reverse its sign such that its resultant is zero. Furthermore, the peel stress at the crack tip should be compressive in order to balance the moment of the compressive resultant force N_y.

References

1. Pagano, N.J. and Pipes, R.B., "Some Observations on the Interlaminar Strength of Composite Laminates," International Journal of Mechanical Sciences, Vol. 15, 1973, pp 679-688.

2. O'Brien, T.K., "Characterization of Delamination Onset and Growth in a Composite Laminate," Damage in Composite Materials, ASTM STP 775, K.L. Reifsnider, Editor, American Society fo Testing and Materials, Philadelphia, 1982, pp 140-167.

3. O'Brien, T.K., "Mixed-Mode Strain-Energy-Release Rate Effects on Edge Delamination of Composites," Effects of Defects in Composite Materials, ASTM STP 836, American Society for Testing and Materials, Philadelphia, 1984, 125-142.

4. O'Brien, T.K. and Raju, I.S., "Strain-Energy-Release Rate Analysis of Delamination Around on Open Hole in Composite Laminates, "AIAA Paper 84-0961, presented at the 25th AIAA/ASME/ASCE/AHS Structures, Structural Dynamics and Materials Conference, May 14-16, 1984, Palm Springs, California.

5. Whitney, J.M. and Knight, Marvin, "A Modified Free-Edge Delamination Specimen," Delamination and Debonding of Materials, ASTM STP 876, W.S. Johnson, Ed., American Society for Testing and Materials, Philadelphia, 1985, pp. 298-314.

6. Whitney, J.M., "Stress Analysis of a Mode I Edge Delamination Specimen for Composite Materials," AIAA Paper 85-0611, presented at the 26th AIAA/ASME/ASCE/AHS Structures, Structural Dynamics and Materials Conference, April 15-17, 1985, Orlando, Florida.

7. Johnson, W.R. and Mangalgiri, P.D., "Influence of the resin on Interlaminar Mixed-Mode Fracture," NASA TM 87571, July, 1985, Langley Research Center, Hampton, Virginia.

8. Russell, A.J. and Street, K.N., "Moisture and Temperature Effects on the Mixed-Mode Delamination Fracture of Unidirectional Graphite/Epoxy, "Delamination and Debonding of Materials, ASTM STP 876, W.S. Johnson, Ed., American Society for Testing and Materials, Philadelphia, 1985, pp. 349-370.

9. Armanios, E.A. "New Methods of Sublaminate Analysis for Composite Structures and Applications to Fracture Processes," Ph.D. Thesis, Georgia Institute of Technology, March 1985.

10. Irwin, G.R., "Fracture," Handbuk der Physik, Vol. V, Springer-Verlag, (1958), pp. 551.

11. Rybicki, E.F. and Kanninen, M.F., "A Finite Element Calculation of Stress Intensity Factors by a Modified Crack Closure Integral," Eng. Fract. Mech., Vol 9, 1977, pp. 931-938.

Table I. Material Properties and Geometry of the ED Specimen

E_{11} = 134 Gpa

E_{22} = 10.2 GPa

G_{12} = 5.52 GPa

ν_{12} = 0.3

$G_{31} = G_{23}$ = 3.1 GPa

Ply thickness (h) = 0.14×10^{-3} m

Semi-Width (b) = 140h

Crack length (a) = 6h

Table II. Comparison of Characteristic Equation Coefficients

Laminate	$E_8 \times 10^{-9}$	$E_6 \times 10^{-9}$	$E_4 \times 10^{-9}$	$E_2 \times 10^{-9}$	$E_o \times 10^{-9}$
$[15_{\uparrow}/60/-75/-30]_s$	0.143	-6.940×10^{3}	9.089×10^{7}	-3.132×10^{11}	3.193×10^{14}
$[-35/55_{\uparrow}/10/-80]_s$	2.282	-6.049×10^{4}	4.614×10^{8}	-1.155×10^{12}	5.676×10^{14}
$[40/-50/85_{\uparrow}/-5]_s$	0.095	-6.389×10^{3}	1.071×10^{8}	-4.096×10^{11}	3.193×10^{14}

Table III. Comparison of the Characteristic Roots for a $[35/80_{\uparrow}/-55/-10]_s$ Layup

Model	s_{x_1}	s_{y_1}	s_{x_2}	s_{y_2}
Coupled	5547	4286	2714	2438
Uncoupled	5538	3737	2427	2108
Membrane			2802	2162

Table IV. COMPARISON OF ENERGY RELEASE COMPONENTS IN ED SPECIMENS (a = 6h, b = 140h)

STACKING SEQUENCE	G_I/G_T		G_{II}/G_T		G_{III}/G_T	
	PRESENT	FEM	PRESENT	FEM	PRESENT	FEM
$[35/-35/0_{\uparrow}/90]_s$	86.5	90.0	13.3	10.0	0.2	0.0
$[35/0/-35_{\uparrow}/90]_s$	59.5	58.0	40.5	42.0	0.0	0.0
$[0/35/-35_{\uparrow}/90]_s$	26.3	22.0	73.7	78.0	0.0	0.0
$[30/-60_{\uparrow}/75/-15]_s$	9.6	16.9	4.9	0.4	85.5	81.7
$[35/80_{\uparrow}/-55/-10]_s$	13.5	7.5	1.9	2.7	84.6	89.8
$[-35/55_{\uparrow}/10/-80]_s$	18.5	20.6	14.8	11.7	66.7	67.7

Table V. $[0/90/\pm 45]_s$ Laminate with Circular Hole- Edge Delamination at + 45/-45 Interface (a = 6h, b= 140h, $\varepsilon = 10^{-6}$)

ANGULAR POSITION	STACKING SEQUENCE	G_I/G_T		G_{II}/G_T		G_{III}/G_T		$10^6 G_T$	
		PRESENT	FEM	PRESENT	FEM	PRESENT	FEM	PRESENT	FEM
50^o	$[40/-50/85/\underset{\uparrow}{-5}]_s$	57.65	53.65	1.03	2.96	41.31	43.39	2.83	2.93
55^o	$[35/-55/80/\underset{\uparrow}{-10}]_s$	30.59	24.11	2.33	3.45	67.08	72.44	4.94	5.11
60^o	$[30/-60/75/\underset{\uparrow}{-15}]_s$	18.97	10.98	4.19	5.21	76.85	83.80	6.29	6.51
65^o	$[25/-65/70/\underset{\uparrow}{-20}]_s$	10.47	3.40	6.81	7.86	82.72	88.74	6.73	6.95

Table VI. $[0/90/\pm 45]_s$ Laminate with Circular Hole- Edge Delamination at 90/45 Interface (a = 6h, b = 140h, $\varepsilon = 10^{-6}$)

ANGULAR POSITION	STACKING SEQUENCE	G_I/G_T		G_{II}/G_T		G_{III}/G_T		$10^6\ G_T$	
		PRESENT	FEM	PRESENT	FEM	PRESENT	FEM	PRESENT	FEM
-70^o	$[-20/70/\underset{\uparrow}{25}/-65]_s$	10.33	1.80	1.01	-2.20	88.66	100.40	6.11	6.37
-65^o	$[-25/65/\underset{\uparrow}{20}/-70]_s$	12.59	5.80	0.17	-3.18	87.24	97.38	6.11	6.36
-60^o	$[-30/60/\underset{\uparrow}{15}/-75]_s$	15.11	11.87	3.73	0.86	81.16	87.26	5.42	5.64
-55^o	$[-35/55/\underset{\uparrow}{10}/-80]_s$	18.56	20.64	14.79	11.66	66.65	67.71	4.10	4.27
-50^o	$[-40/50/\underset{\uparrow}{5}/-85]_s$	24.34	33.18	42.16	36.48	33.50	30.34	2.60	2.70
-45^o	$[-45/45/\underset{\uparrow}{0}/90]_s$	27.87	35.07	72.13	65.40	0.00	-0.46	1.88	1.95

Table VII. [0/90/ ± 45] Laminate with Circular Hole- Edge Delamination at 0/90 Interface (a = 6h, b - 140h, ε - 10^{-6})

ANGULAR POSITION	STACKING SEQUENCE	G_I/G_T		$G_{II}G_T$		G_{III}/G_T		$10^6\ G_T$	
		PRESENT	FEM	PRESENT	FEM	PRESENT	FEM	PRESENT	FEM
-85^o	$[-5_{\uparrow}/85/40/-50]_s$	3.40	0.22	0.08	0.34	96.52	99.44	1.26	1.40
-80^o	$[-10_{\uparrow}/80/35/-55]_s$	4.08	0.40	0.40	0.54	95.52	99.06	3.41	3.74
-75^o	$[-15_{\uparrow}/75/30/-60]_s$	5.06	0.86	0.98	1.07	93.96	98.07	4.88	5.33
-70^o	$[-20_{\uparrow}/70/25/-65]_s$	6.29	1.59	1.85	1.97	91.86	96.43	5.51	6.03
-65^o	$[-25_{\uparrow}/65/20/-70]_s$	7.73	2.49	3.04	3.36	89.24	94.15	5.53	6.03
-60^o	$[-30_{\uparrow}/60/15/-75]_s$	9.25	3.37	4.55	5.35	86.21	91.29	5.10	5.49
-55^o	$[-35_{\uparrow}/55/10/-80]_s$	10.62	4.07	6.34	7.95	83.04	87.98	4.30	4.56
-50^o	$[-40_{\uparrow}/50/5/-85]_s$	11.58	4.52	8.26	10.92	80.16	84.56	3.27	3.36
-45^o	$[-45_{\uparrow}/45/0/90]_s$	11.89	4.64	9.87	13.48	78.23	81.88	2.14	2.10

Table VIII. $[45/90/-45/0]_s$ Laminate with Circular Hole- Edge Delamination at -45/0 Interface ($a = 6h$, $b = 140h$, $\varepsilon = 10^{-6}$)

ANGULAR POSITION	STACKING SEQUENCE	G_I/G_T		G_{II}/G_T		G_{III}/G_T		$10^6 G_T$		
		PRESENT	FEM	PRESENT	FEM	PRESENT	FEM	PRESENT	FEM	O'BRIEN
-85^o	$[40/85/-50/\underset{\uparrow}{-5}]_s$	2.57	2.68	0.00	-1.28	97.43	98.61	1.28	1.25	0.87
-80^o	$[35/80/-55/\underset{\uparrow}{-10}]_s$	0.07	2.28	0.00	-1.27	99.93	98.99	3.43	3.47	3.58
-75^o	$[30/75/-60/\underset{\uparrow}{-15}]_s$	0.57	1.81	0.00	-1.09	99.43	99.27	4.91	5.00	5.12
-70^o	$[25/70/-65/\underset{\uparrow}{-20}]_s$	1.14	1.25	0.41	-0.44	98.44	99.19	5.55	5.68	5.78
-65^o	$[20/65/-70/\underset{\uparrow}{-25}]_s$	1.71	0.77	1.47	0.98	96.81	98.25	5.56	5.72	5.79
-60^o	$[15/60/-75/\underset{\uparrow}{-30}]_s$	2.19	0.51	3.49	3.46	94.32	96.03	5.10	5.27	5.31
-55^o	$[10/55/-80/\underset{\uparrow}{-35}]_s$	2.61	0.56	6.85	7.24	90.54	92.20	4.30	4.46	4.48
-50^o	$[5/50/-85/\underset{\uparrow}{-40}]_s$	3.65	1.35	11.88	12.45	84.48	86.20	3.30	3.43	3.44
-45^o	$[0/45/90/\underset{\uparrow}{-45}]_s$	8.18	4.68	18.11	19.12	73.71	76.20	2.31	2.40	2.40
-40^o	$[-5/40/85/\underset{\uparrow}{-50}]_s$	24.36	17.55	21.87	24.38	53.77	58.07	1.56	1.62	1.62
-35^o	$[-10/35/80/\underset{\uparrow}{-55}]_s$	59.94	47.44	14.92	21.58	25.14	30.98	1.20	1.25	1.25
-30^o	$[-15/30/75/\underset{\uparrow}{-60}]_s$	95.57	79.57	0.00	10.90	4.43	9.63	1.22	1.27	1.28

Table IX. [45/90/-45/0] Laminate with Circular Hole- Edge Delamination at 90/-45 Interface (a = 6h, b = 140h, $\varepsilon = 10^{-6}$)

ANGULAR POSITION	STACKING SEQUENCE	G_I/G_T		G_{II}/G_T		G_{III}/G_T		$10^6 G_T$		
		PRESENT	FEM	PRESENT	FEM	PRESENT	FEM	PRESENT	FEM	O'BRIEN
85°	$[50/-85/\underset{\uparrow}{-40}/5]_s$	7.46	3.12	53.34	52.36	38.2	44.52	1.88	1.96	2.03
90°	$[45/90/\underset{\uparrow}{-45}/0]_s$	11.16	7.18	24.00	23.37	64.84	69.45	2.32	2.42	2.43
-85°	$[40/85/\underset{\uparrow}{-50}/-5]_s$	12.94	8.42	7.14	7.84	79.92	83.75	3.20	3.32	3.37
-80°	$[35/80/\underset{\uparrow}{-55}/-10]_s$	13.52	7.54	1.91	2.76	84.56	89.71	4.30	4.45	4.66
-75°	$[30/75/\underset{\uparrow}{-60}/-15]_s$	13.74	6.02	0.98	1.67	85.28	92.30	5.28	5.46	5.83
-70°	$[25/70/\underset{\uparrow}{-65}/-20]_s$	13.74	4.52	0.46	1.63	85.80	93.85	5.86	6.05	6.49
-65°	$[20/65/\underset{\uparrow}{-70}/-25]_s$	12.34	3.38	0.00	1.52	87.66	95.20	5.88	6.07	6.40
-60°	$[15/60/\underset{\uparrow}{-75}/-30]_s$	8.76	2.43	0.00	0.70	91.24	96.87	5.31	5.48	5.83
-55°	$[10/55/\underset{\uparrow}{-80}/-35]_s$	4.64	2.13	0.00	-0.94	95.36	98.82	4.26	4.40	4.66
-50°	$[5/50/\underset{\uparrow}{-85}/-40]_s$	5.63	2.73	0.00	-0.62	94.37	97.89	3.08	3.18	3.37
-45°	$[0/45/\underset{\uparrow}{90}/-45]_s$	2.42	5.31	21.43	11.18	76.15	83.85	2.23	2.32	2.43
-40°	$[-5/40/\underset{\uparrow}{85}/-50]_s$	16.78	10.03	51.48	38.02	31.74	51.95	1.89	2.38	2.03
-35°	$[-10/35/\underset{\uparrow}{80}/-55]_s$	20.92	19.22	68.30	58.69	10.69	22.09	1.90	2.43	2.01
-45°	$[-15/30/\underset{\uparrow}{75}/-60]_s$	29.51	32.61	67.58	61.72	2.92	5.68	2.00	2.43	2.10

Table X. $[45/90/-45/0]_s$ Laminate with Circular Hole- Edge Delamination at 45/90 Interface (a = 6h, b = 140h, $\varepsilon = 10^{-6}$)

ANGULAR POSITION	STACKING SEQUENCE	G_I/G_T PRESENT	G_I/G_T FEM	G_{II}/G_T PRESENT	G_{II}/G_T FEM	G_{III}/G_T PRESENT	G_{III}/G_T FEM	$10^6 G_T$ PRESENT	$10^6 G_T$ FEM	$10^6 G_T$ O'BRIEN
85^o	$[50_{\uparrow}/-85/-40/5]_s$	3.28	12.23	10.69	7.00	86.03	80.77	1.10	1.12	1.62
90^o	$[45_{\uparrow}/90/-45/0]_s$	2.89	13.91	10.98	4.08	86.13	82.10	2.14	2.20	2.40
-85^o	$[40_{\uparrow}/85/-50/-5]_s$	2.80	14.20	9.14	1.09	88.05	84.71	3.27	3.39	3.44
-80^o	$[35_{\uparrow}/80/-55/-10]_s$	2.89	13.55	6.9	-1.18	90.21	87.63	4.30	4.46	4.48
-75^o	$[30_{\uparrow}/75/-60/-15]_s$	3.01	12.12	4.85	-2.54	92.14	90.43	5.09	5.27	5.31
-70^o	$[25_{\uparrow}/70/-75/-20]_s$	3.07	10.06	3.17	-3.11	93.76	93.05	5.53	5.71	5.79
-65^o	$[20_{\uparrow}/65/-70/-25]_s$	3.02	7.65	1.9	-3.09	95.08	95.43	5.51	5.67	5.78
-60^o	$[15_{\uparrow}/60/-75/-30]_s$	2.84	5.22	1.00	-2.70	96.16	97.48	4.88	4.99	5.12
-55^o	$[10_{\uparrow}/55/-80/-35]_s$	2.56	3.12	0.41	-2.17	97.02	99.05	3.41	3.47	3.58
-50^o	$[5_{\uparrow}/50/-85/-40]_s$	2.32	1.58	0.08	-1.66	97.60	100.08	1.26	1.25	0.87
-40^o	$[-5_{\uparrow}/40/85/-50]_s$	2.77	0.15	0.07	-0.77	97.16	100.60	1.26	1.42	0.87
-35^o	$[-10_{\uparrow}/35/80/-55]_s$	3.68	-0.30	0.39	-0.01	95.93	100.10	3.41	3.85	3.58
-30^o	$[-15_{\uparrow}/30/75/-60]_s$	4.95	0.37	0.95	1.15	94.1	98.50	4.88	5.49	5.78

Table XI. Resultant Forces for a $[0_{\uparrow}/45/90/-45]_s$ Laminate

Ply Angle	N_y (N/m)	N_{xy} (N/m)
0	-0.008	0
45	2.671	3.031
90	-5.335	0
-45	2.671	-3.031

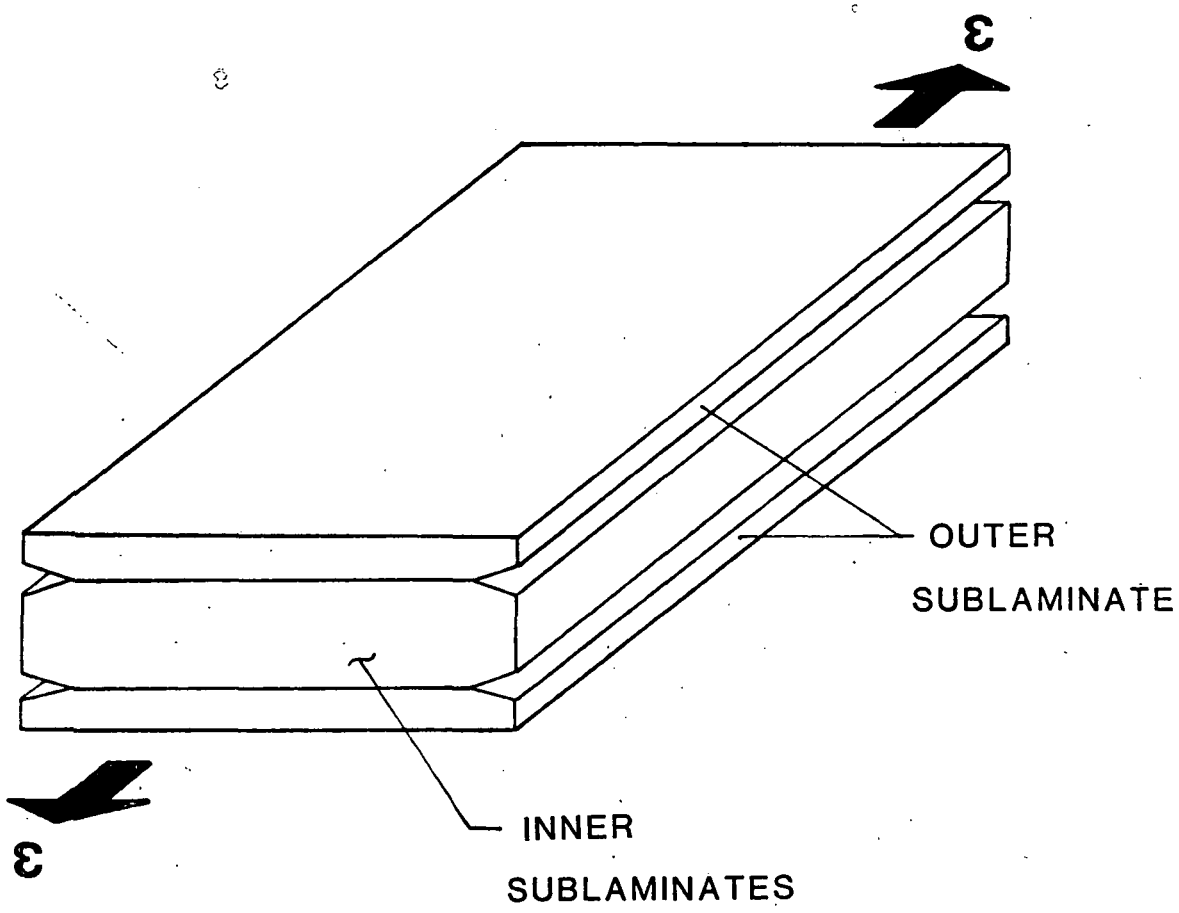

FIGURE 1. THE ED SPECIMEN

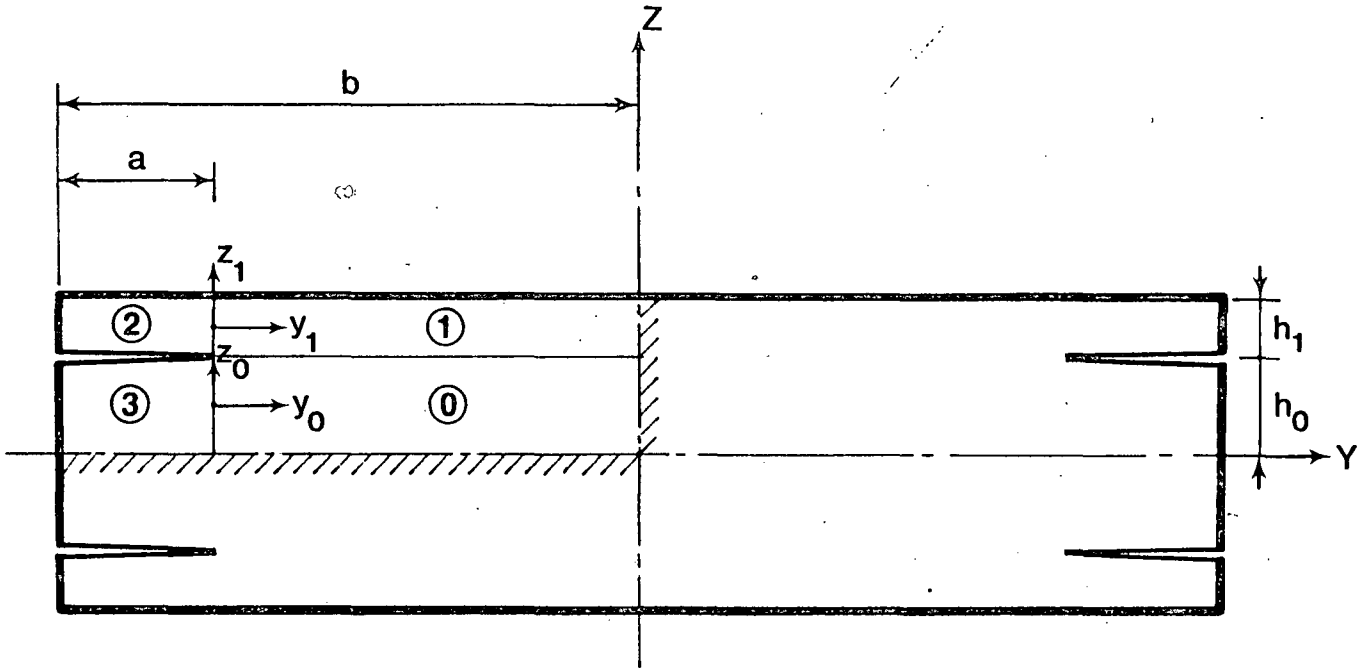

FIGURE 2. SUBLAMINATE DESCRIPTION AND COORDINATE SYSTEMS

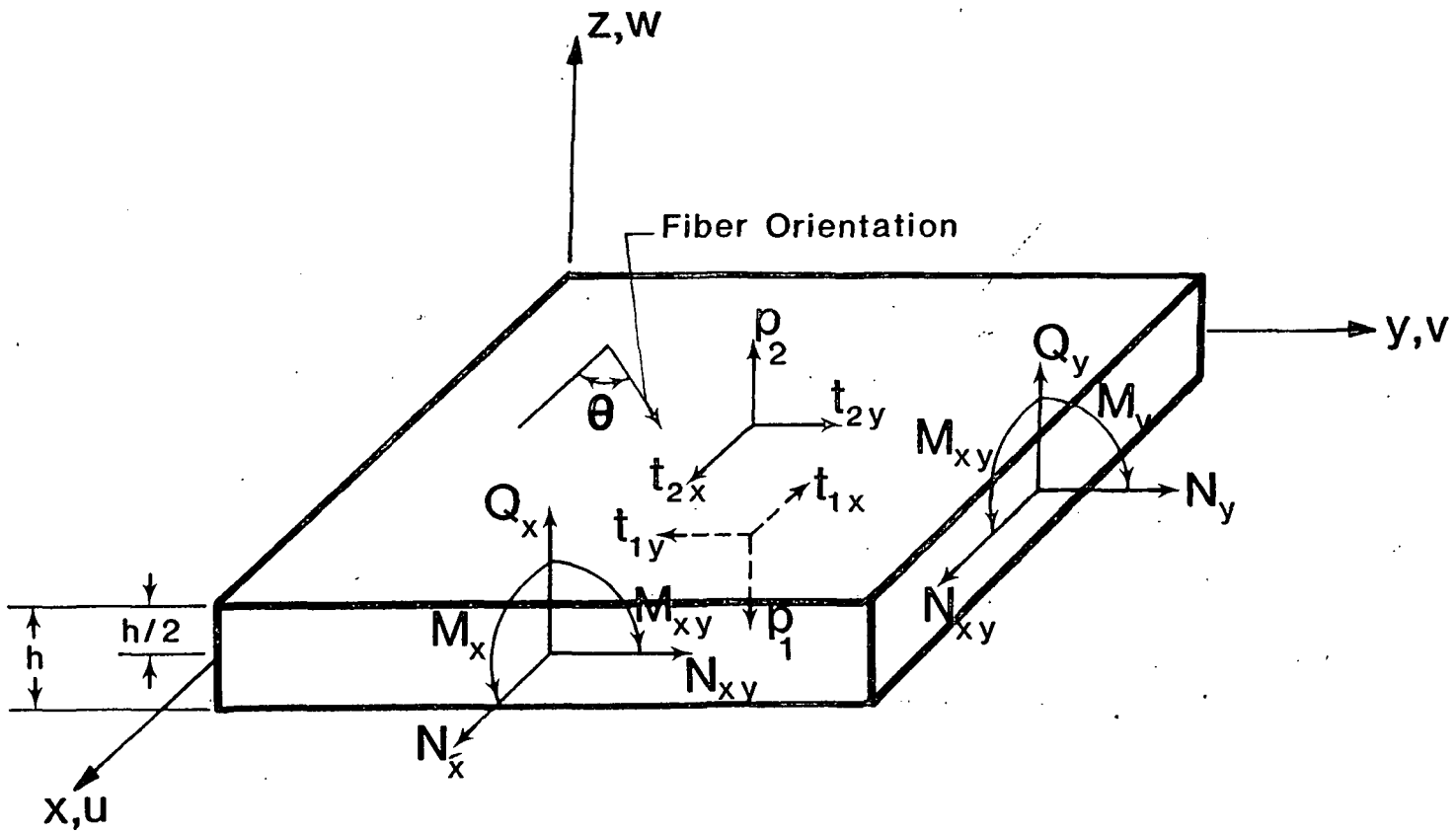

FIGURE 3. NOTATIONS AND SIGN CONVENTION FOR A GENERIC SUBLAMINATE

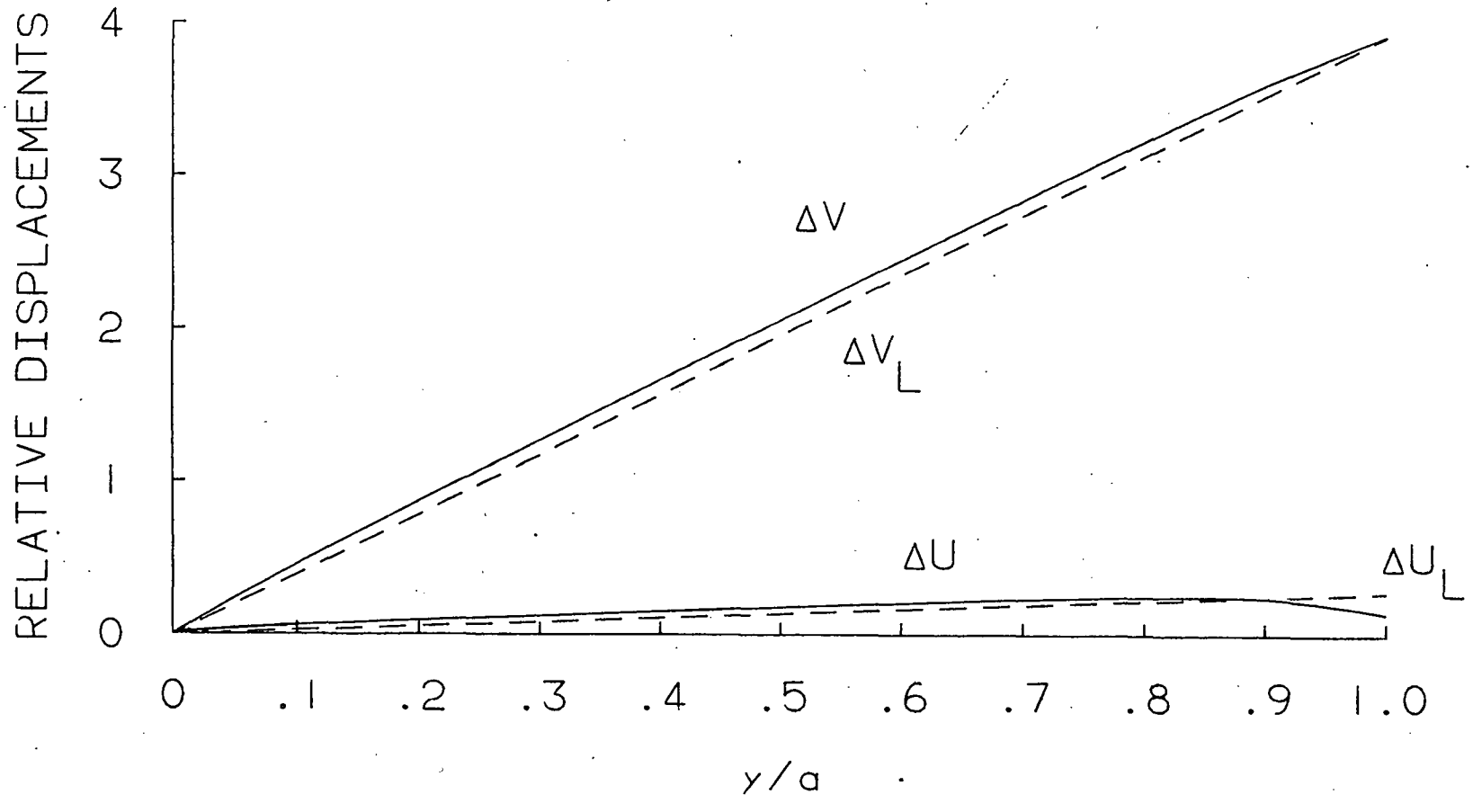

FIGURE. 4 COMPARISON OF RELATIVE DISPLACEMENTS AT THE CRACK SURFACE FOR A [0/35/-35/90]s LAMINATE

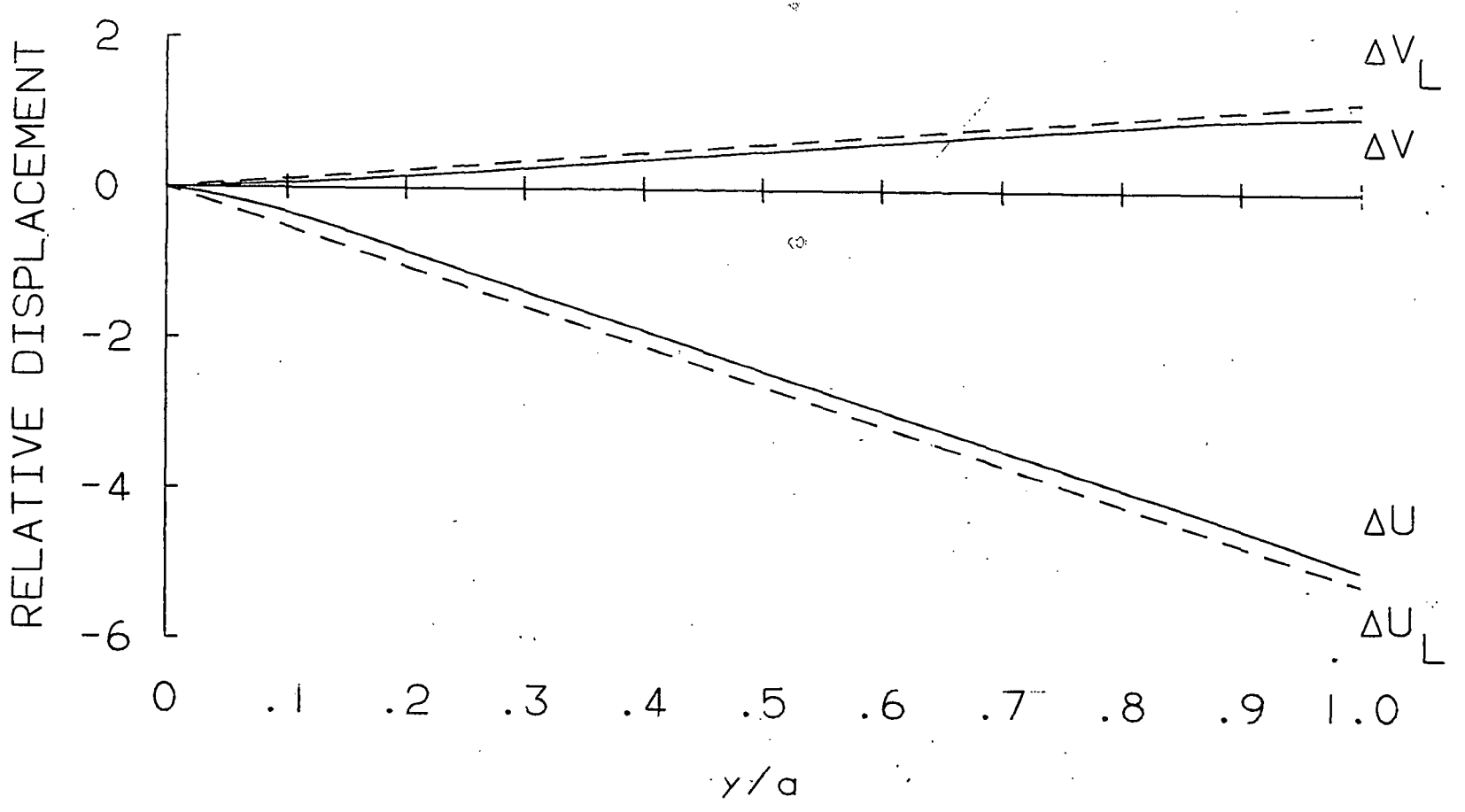

FIGURE 5. COMPARISON OF RELATIVE DISPLACEMENTS AT THE CRACK SURFACE FOR A [-35/55/10/-80]s LAMINATE

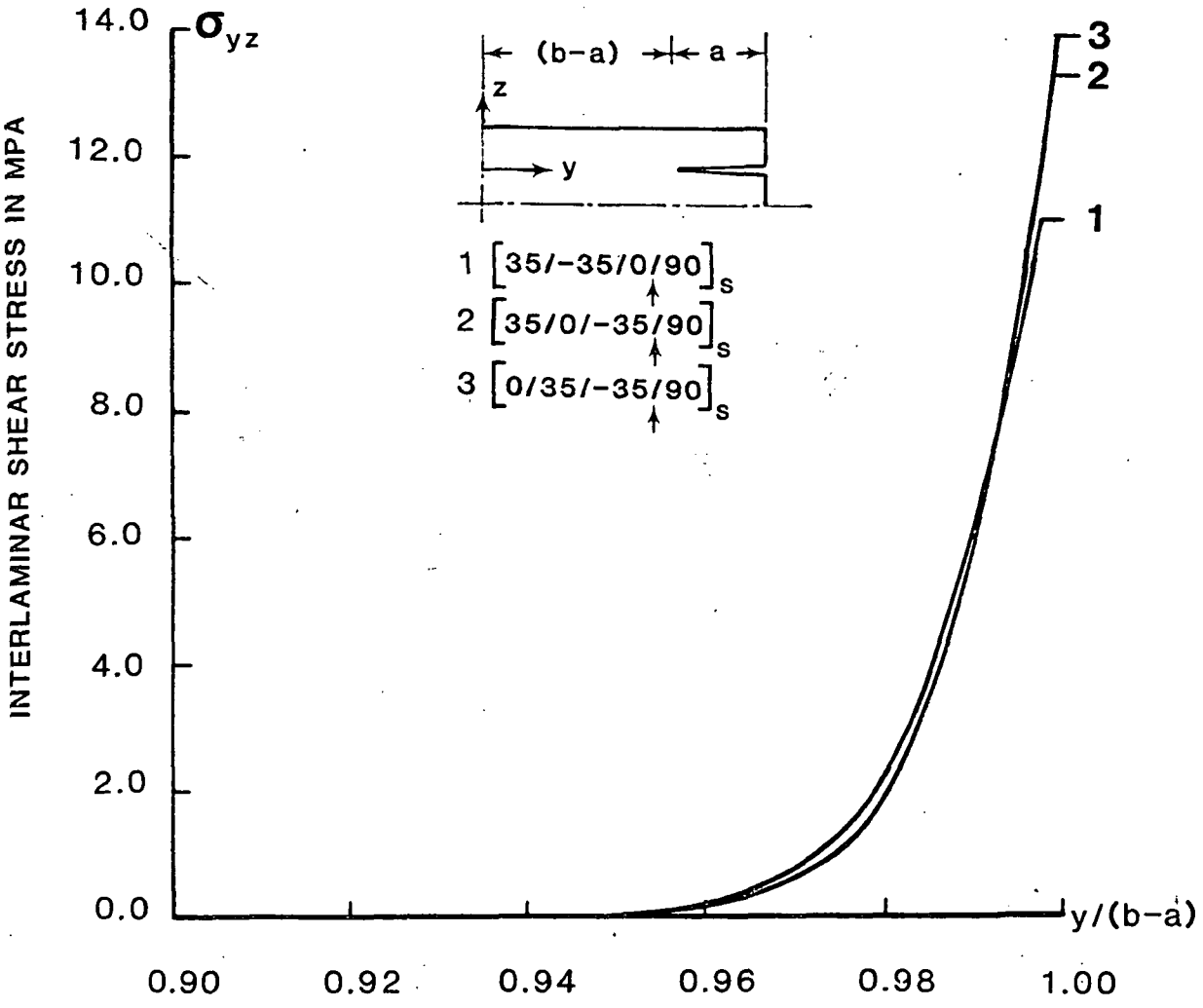

FIGURE 6. COMPARISON OF INTERLAMINAR SHEAR STRESS

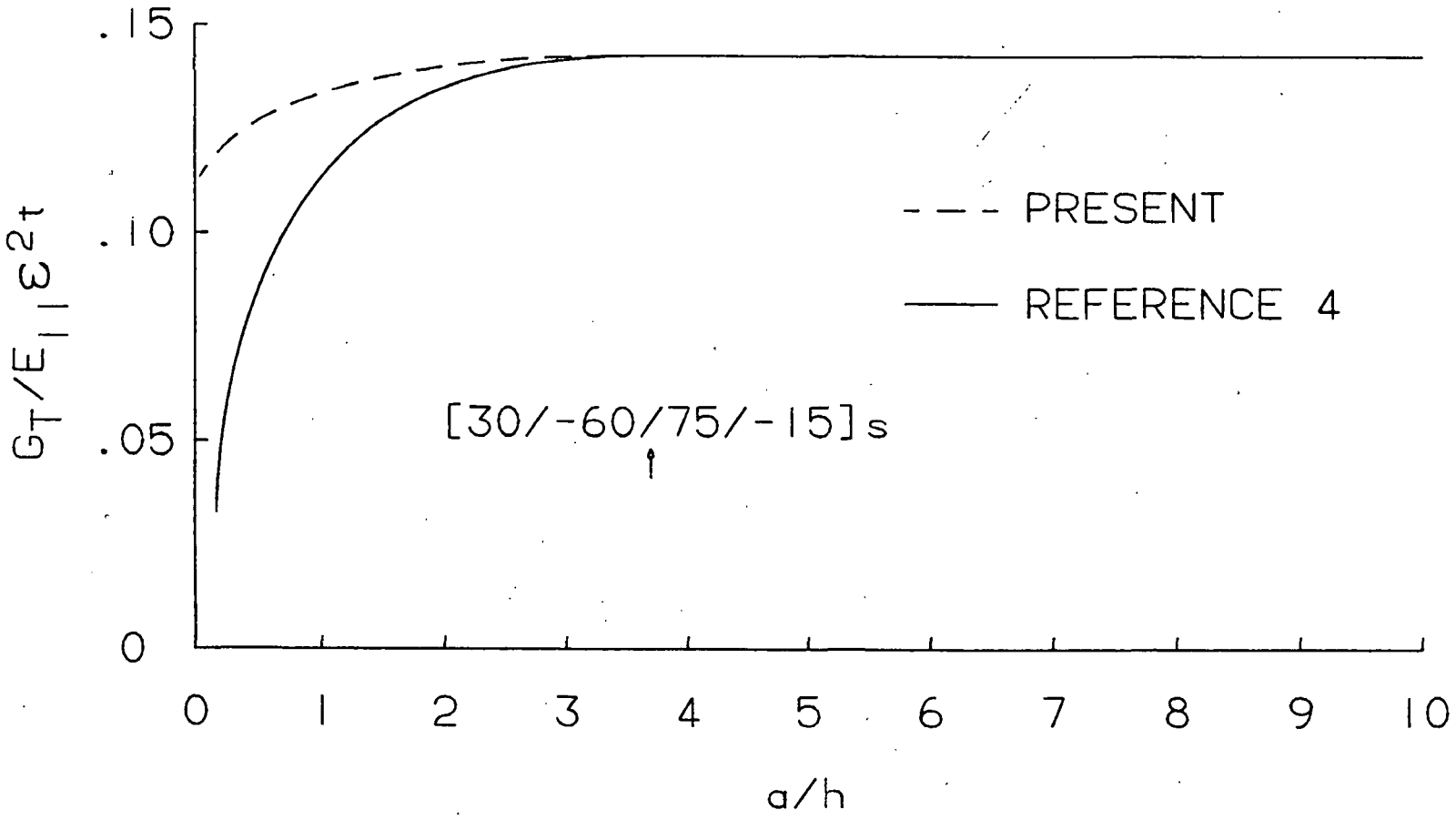

FIGURE 7. NORMALIZED STRAIN-ENERGY-RELEASE RATE AS A FUNCTION OF DELAMINATION SIZE DIVIDED BY PLY THICKNESS

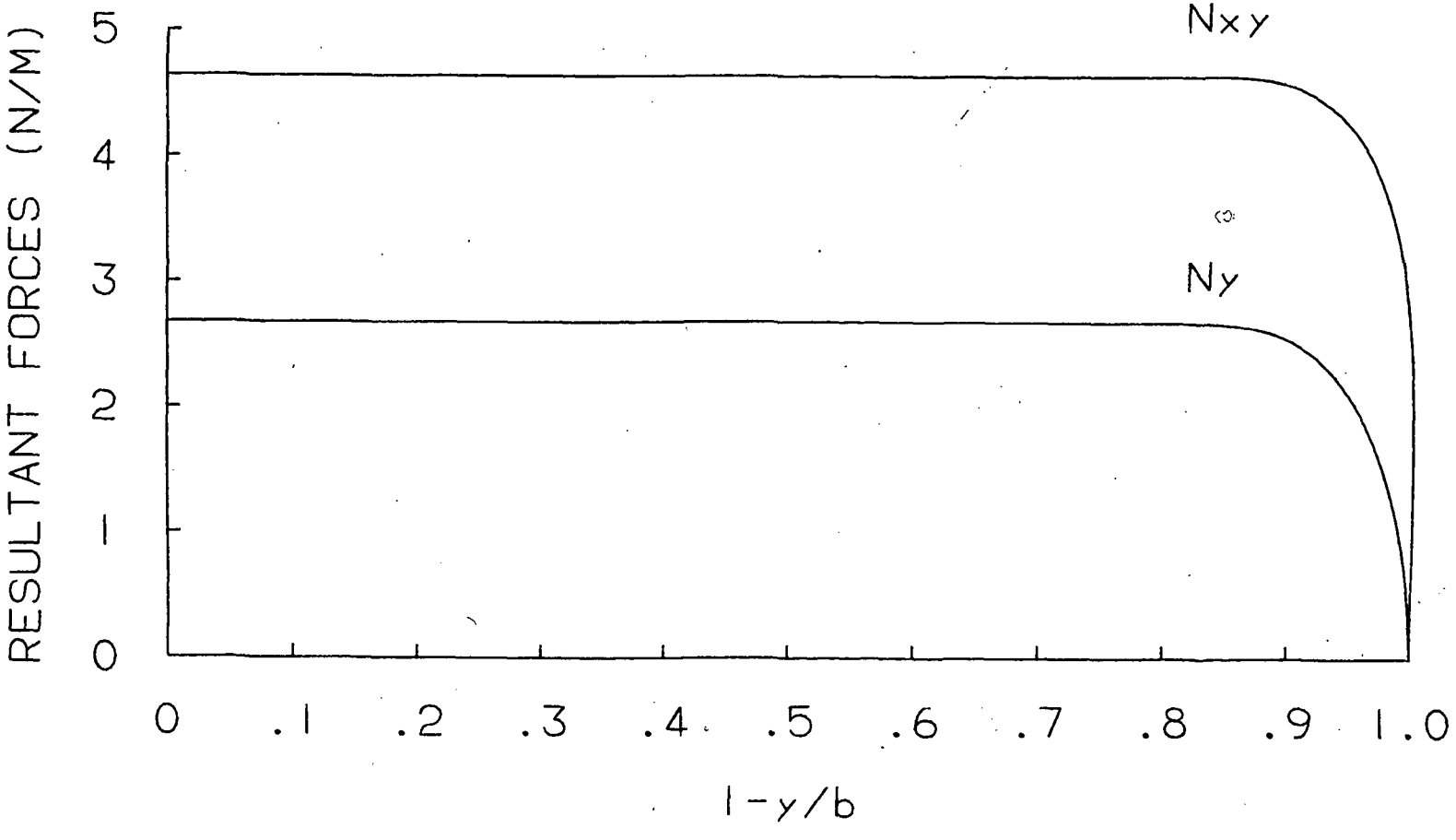

FIGURE 8. RESULTANT FORCE DISTRIBUTION IN A (30/-60/75/-15) LAMINATE

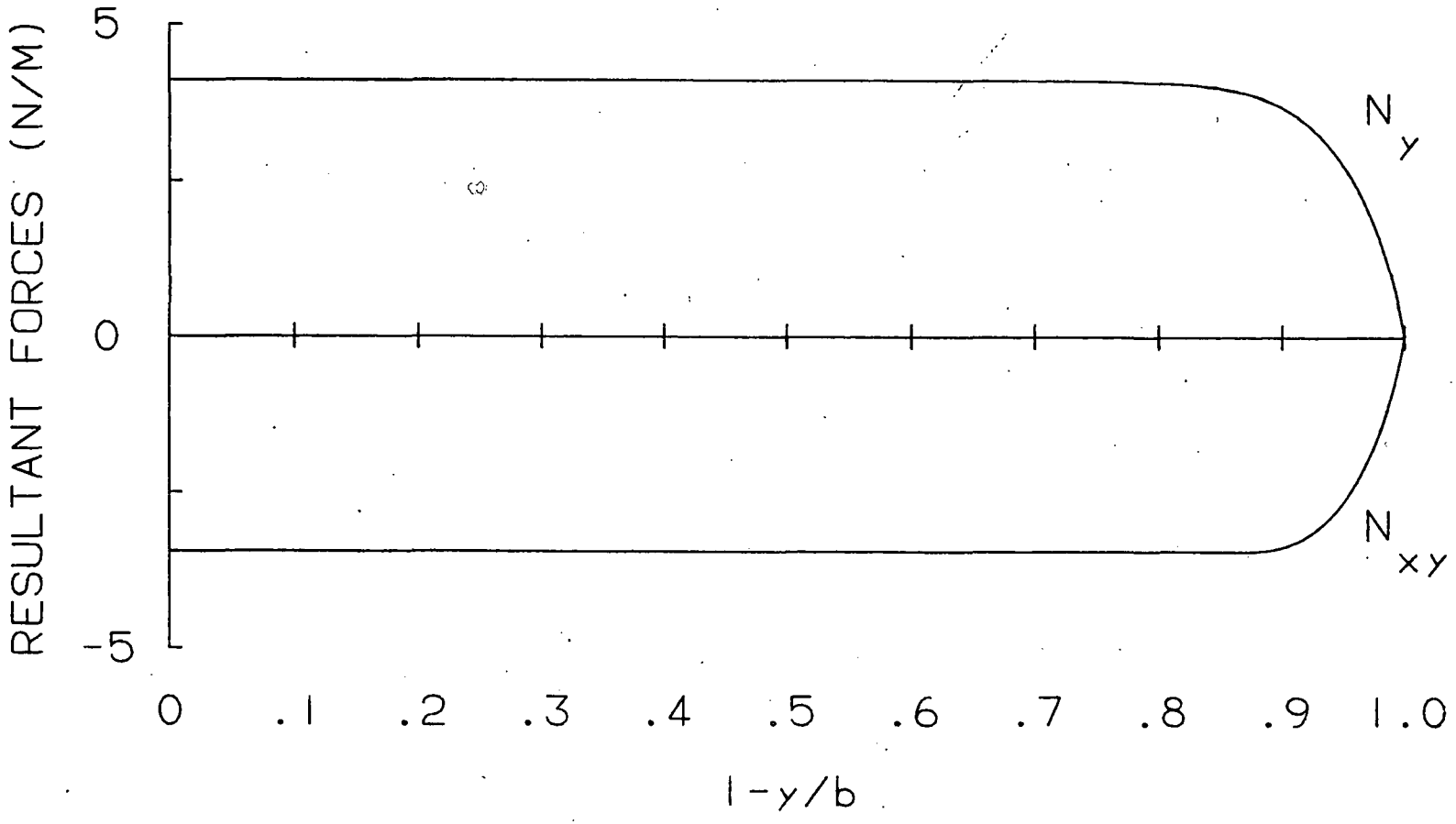

FIGURE 9. RESULTANT FORCE DISTRIBUTION IN A $(-35/55/10/80)_S$ LAMINATE

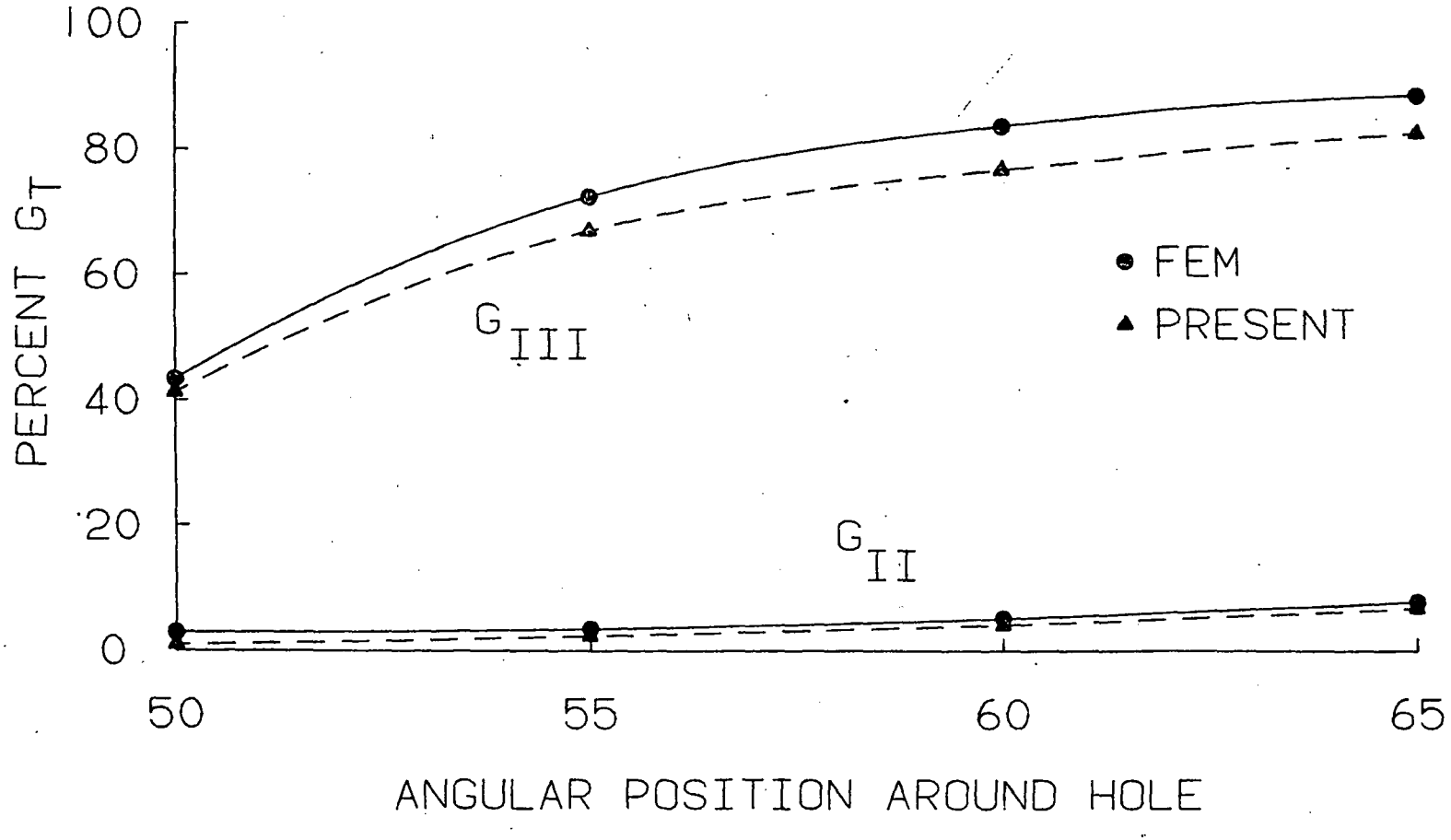

FIGURE 10. [0/90/±45]s LAMINATE WITH CIRCULAR HOLE EDGE DELAMINATION AT +45/-45 INTERFACE

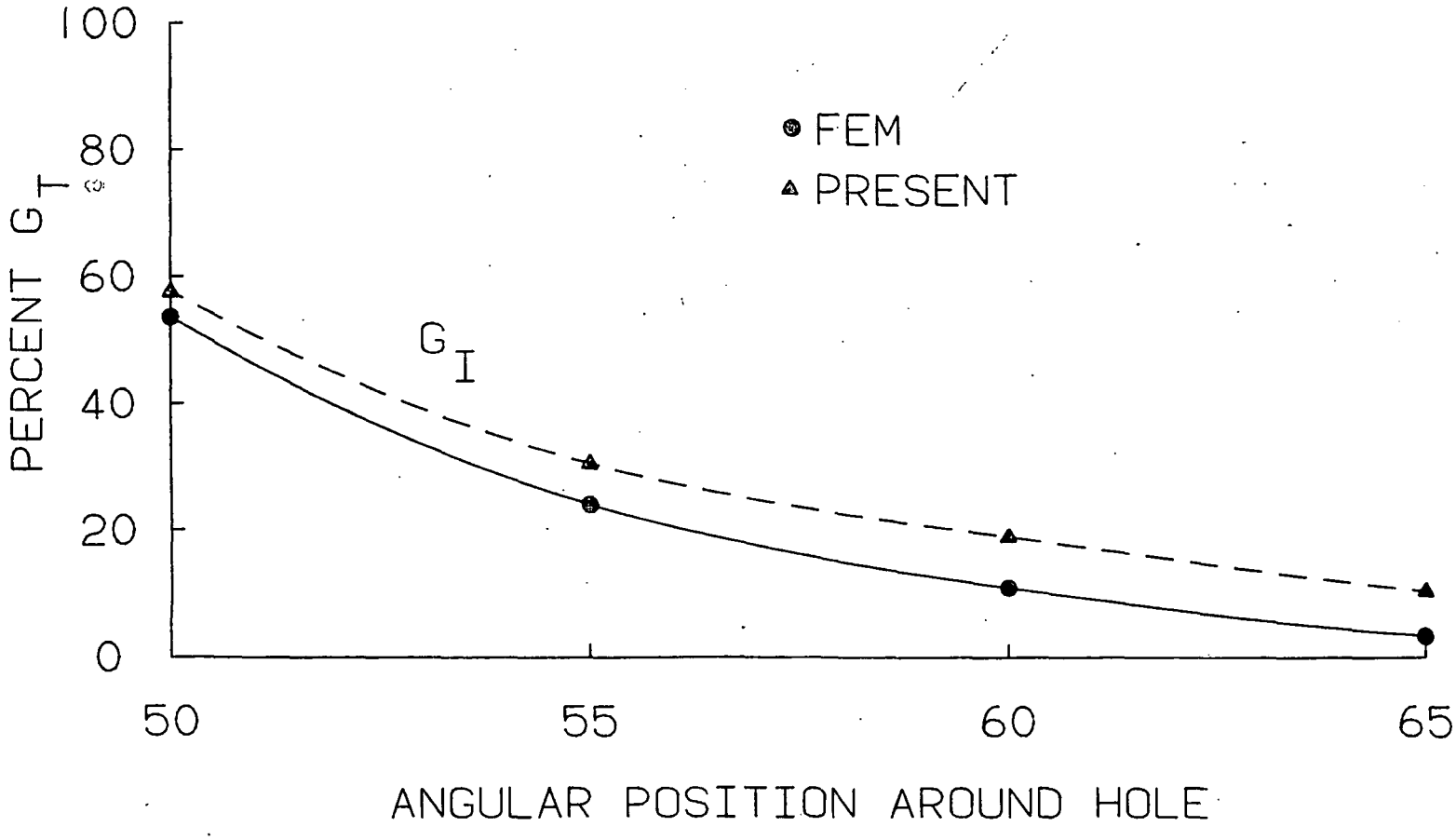

FIGURE 11. [0/90/±45]s LAMINATE WITH CIRCULAR HOLE EDGE DELAMINATION AT +45/-45 INTERFACE

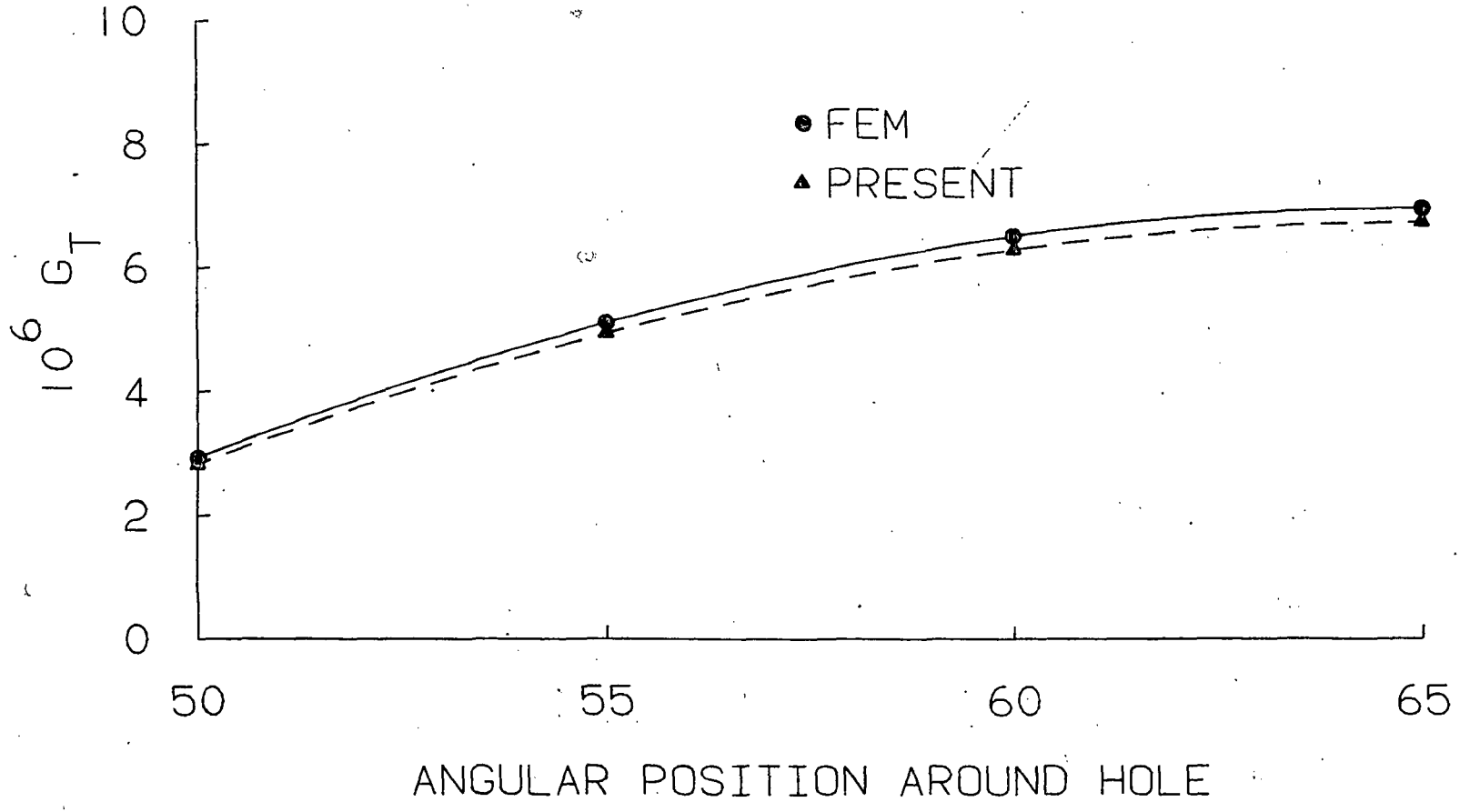

FIGURE 12. [0/90/±45]s LAMINATE WITH CIRCULAR HOLE EDGE DELAMINATION AT +45/-45 INTERFACE

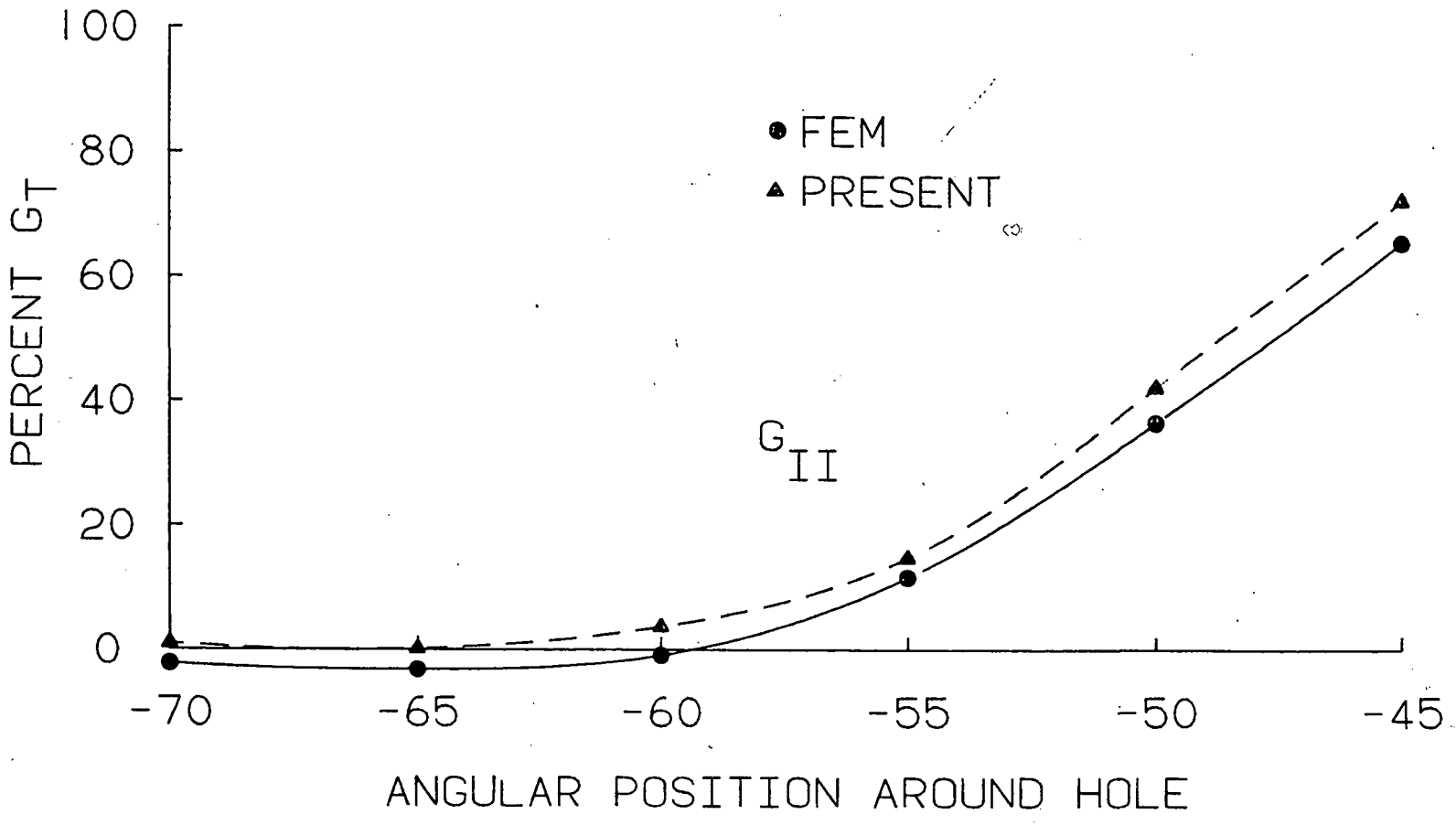

FIGURE 13. [0/90/±45]s LAMINATE WITH CIRCULAR HOLE EDGE DELAMINATION AT 90/+45 INTERFACE

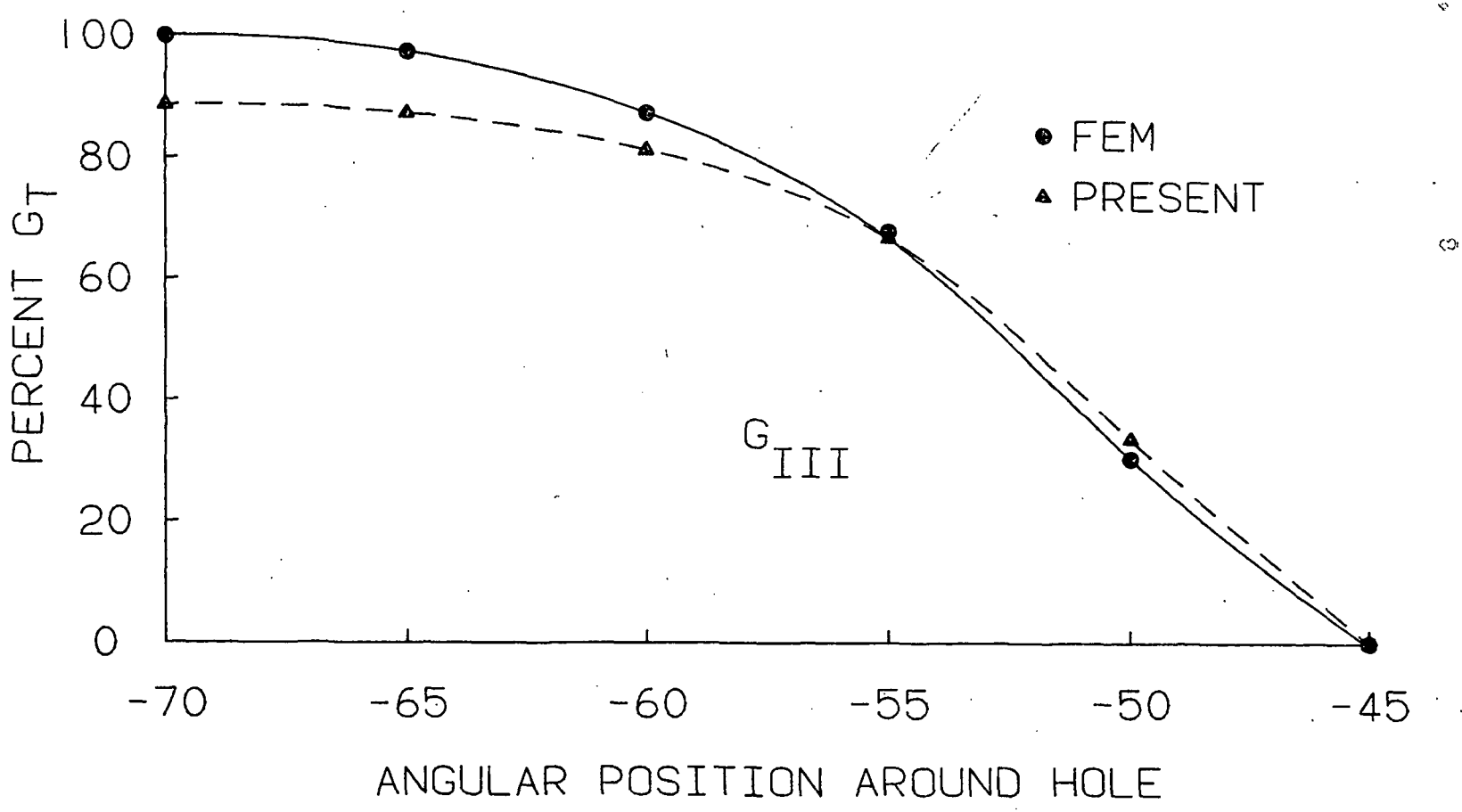

FIGURE 14. [0/90/±45]s LAMINATE WITH CIRCULAR HOLE EDGE DELAMINATION AT 90/+45 INTERFACE

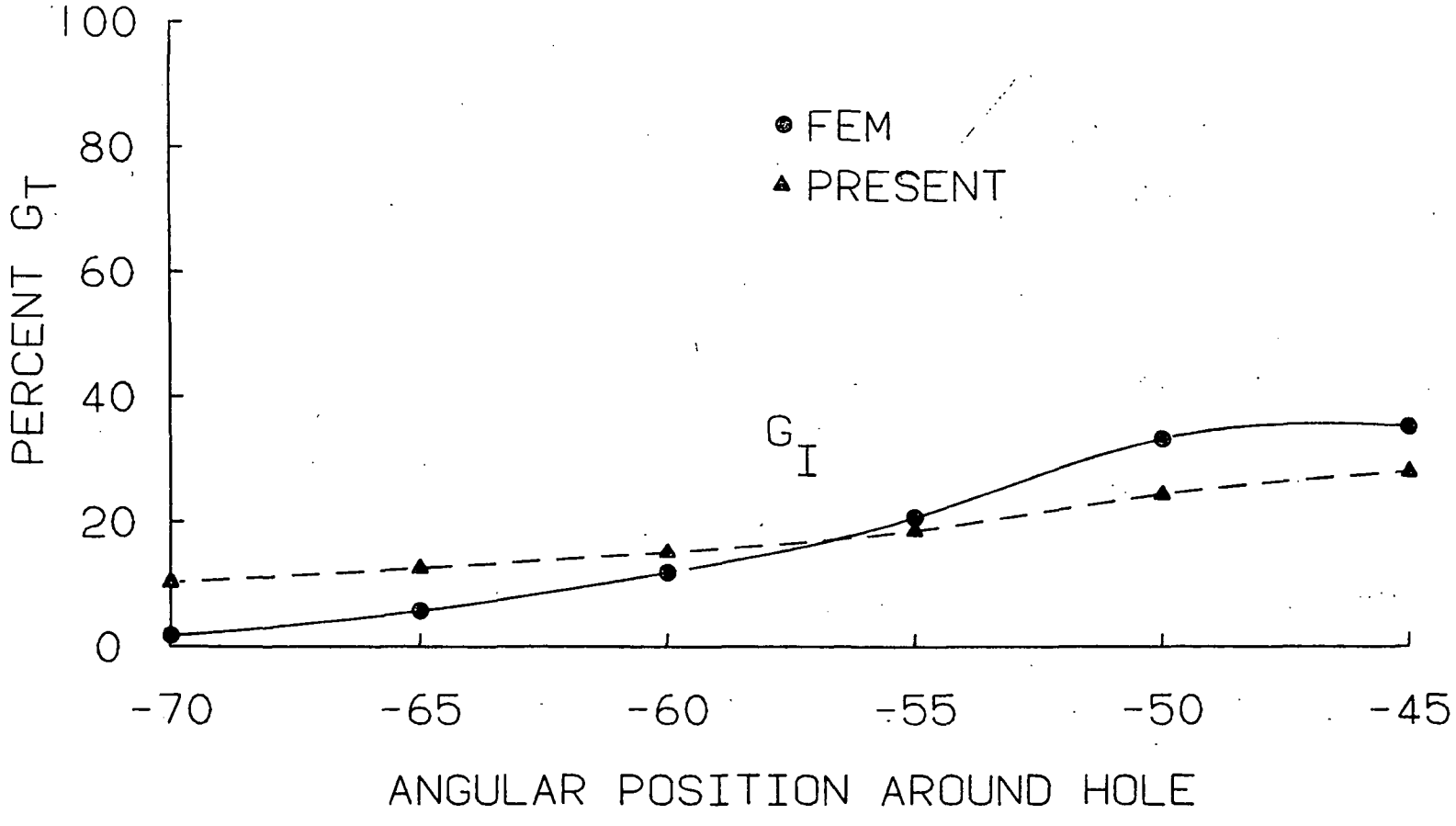

FIGURE 15. [0/90/±45]s LAMINATE WITH CIRCULAR HOLE EDGE DELAMINATION AT 90/+45 INTERFACE

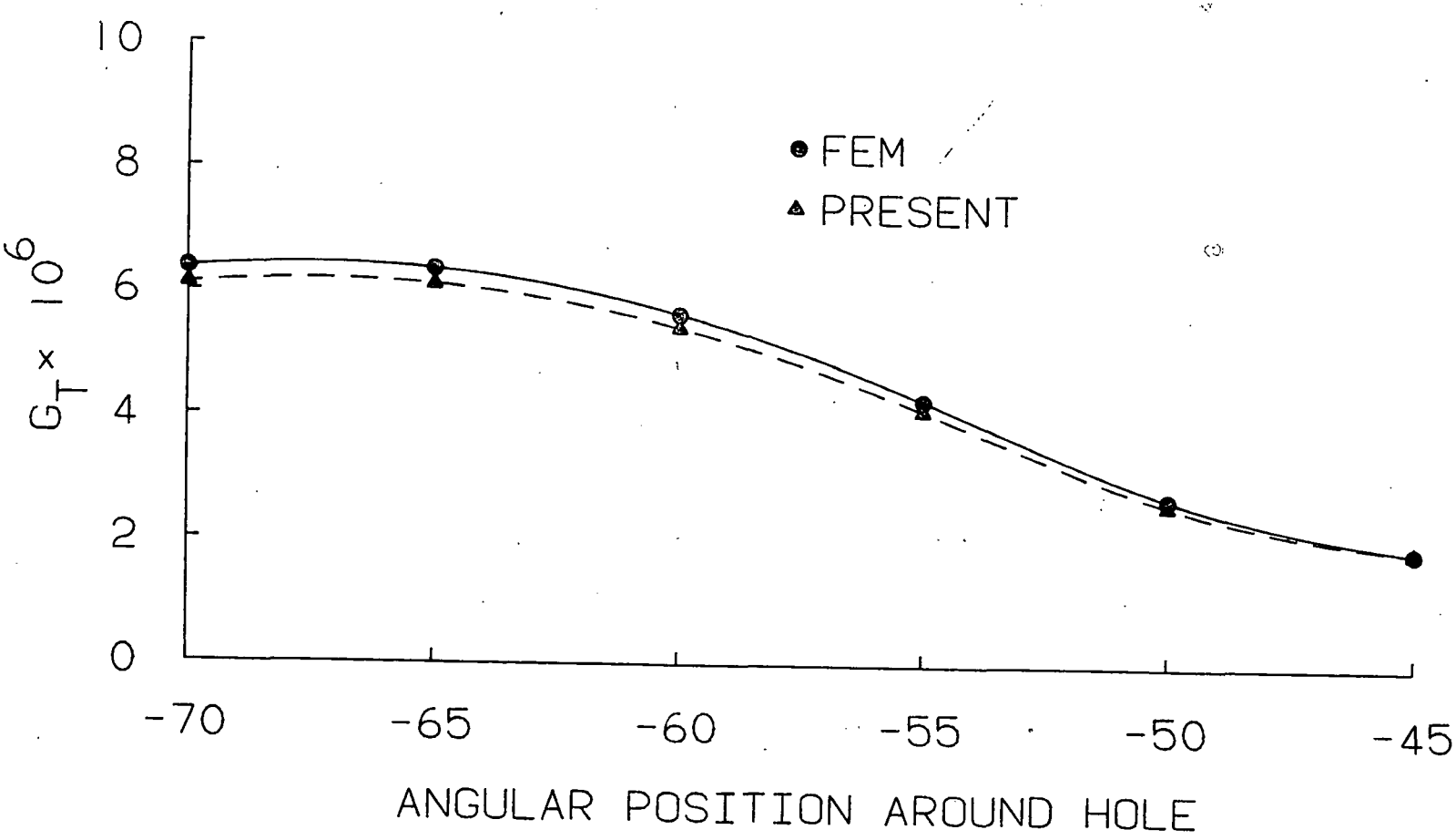

FIGURE 16. [0/90/±45]s LAMINATE WITH CIRCULAR HOLE EDGE DELAMINATION AT 90/+45 INTERFACE

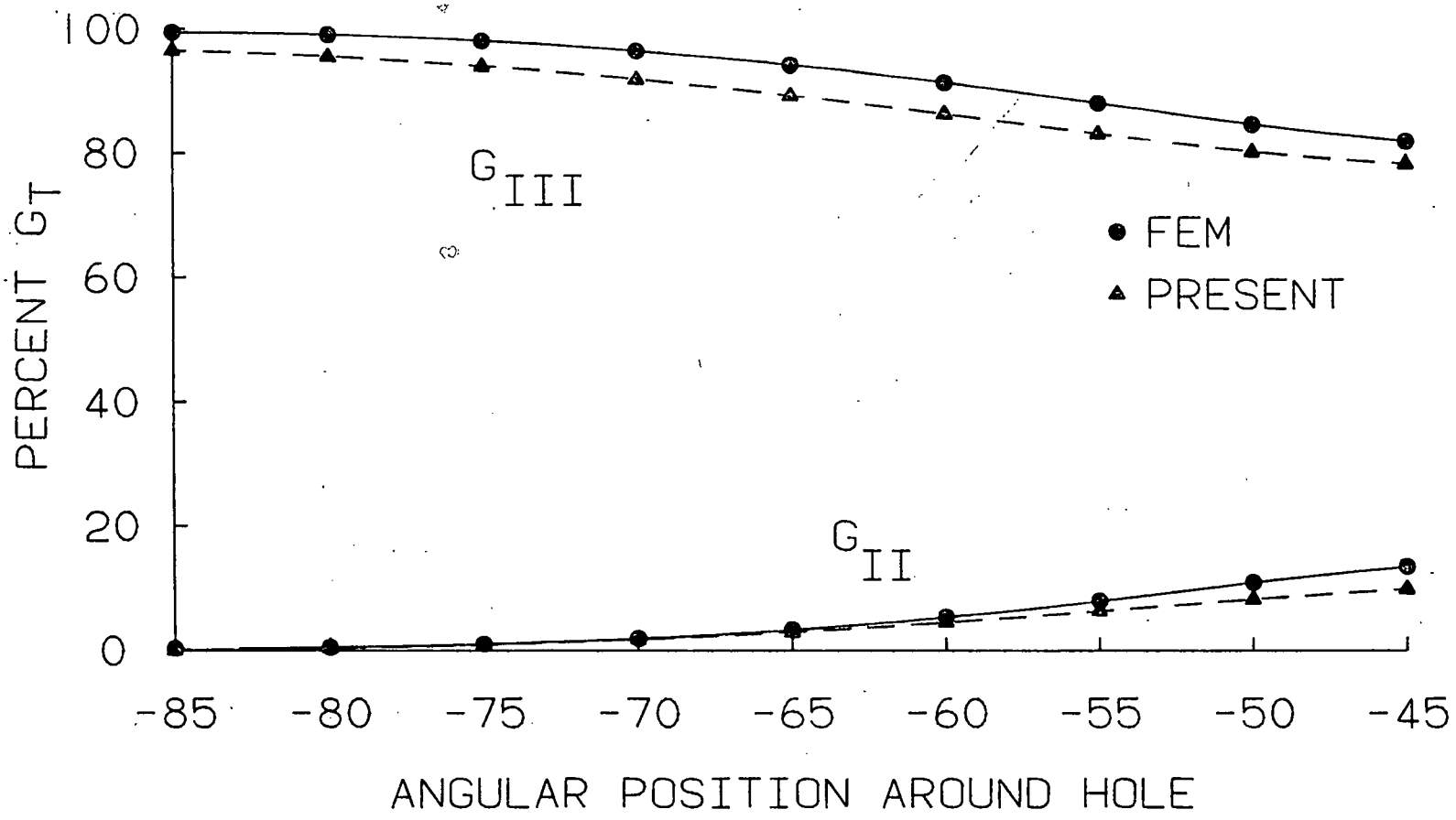

FIGURE 17. [0/90/±45]s LAMINATE WITH CIRCULAR HOLE EDGE DELAMINATION AT 0/90 INTERFACE

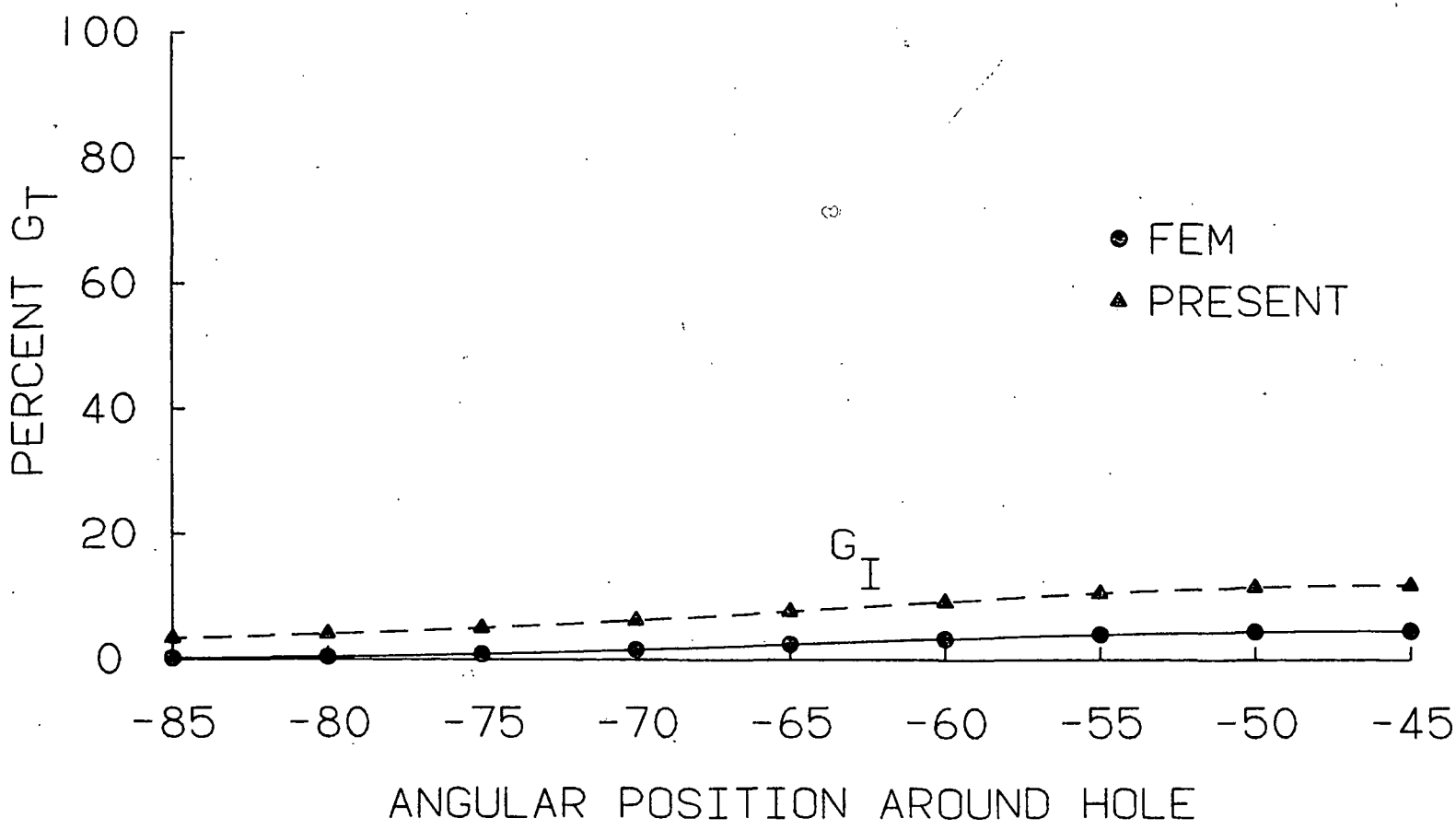

FIGURE 18. [0/90/±45]s LAMINATE WITH CIRCULAR HOLE EDGE DELAMINATION AT 0/90 INTERFACE

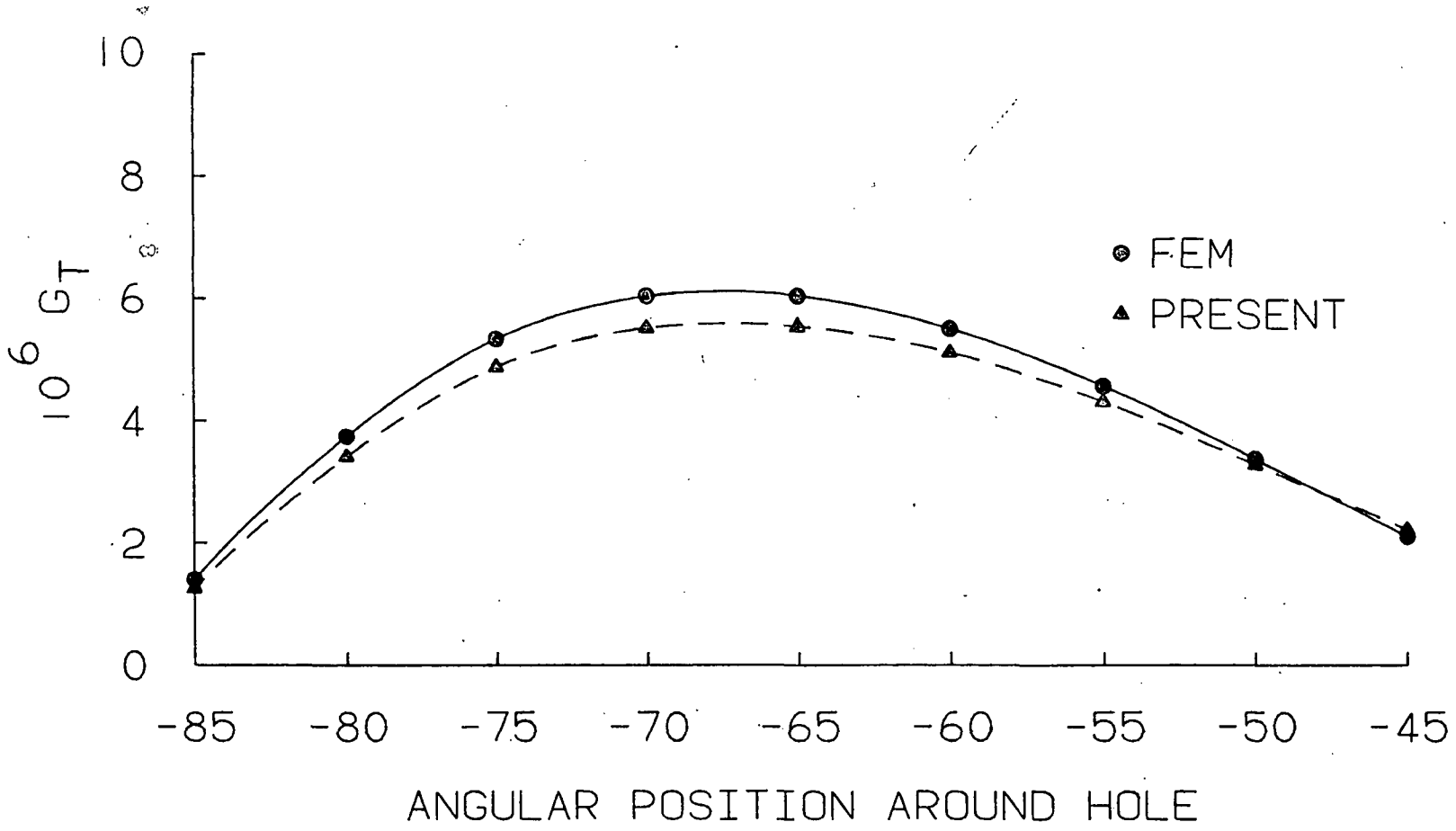

FIGURE 19. [0/90/±45]s LAMINATE WITH CIRCULAR HOLE EDGE DELAMINATION AT 0/90 INTERFACE

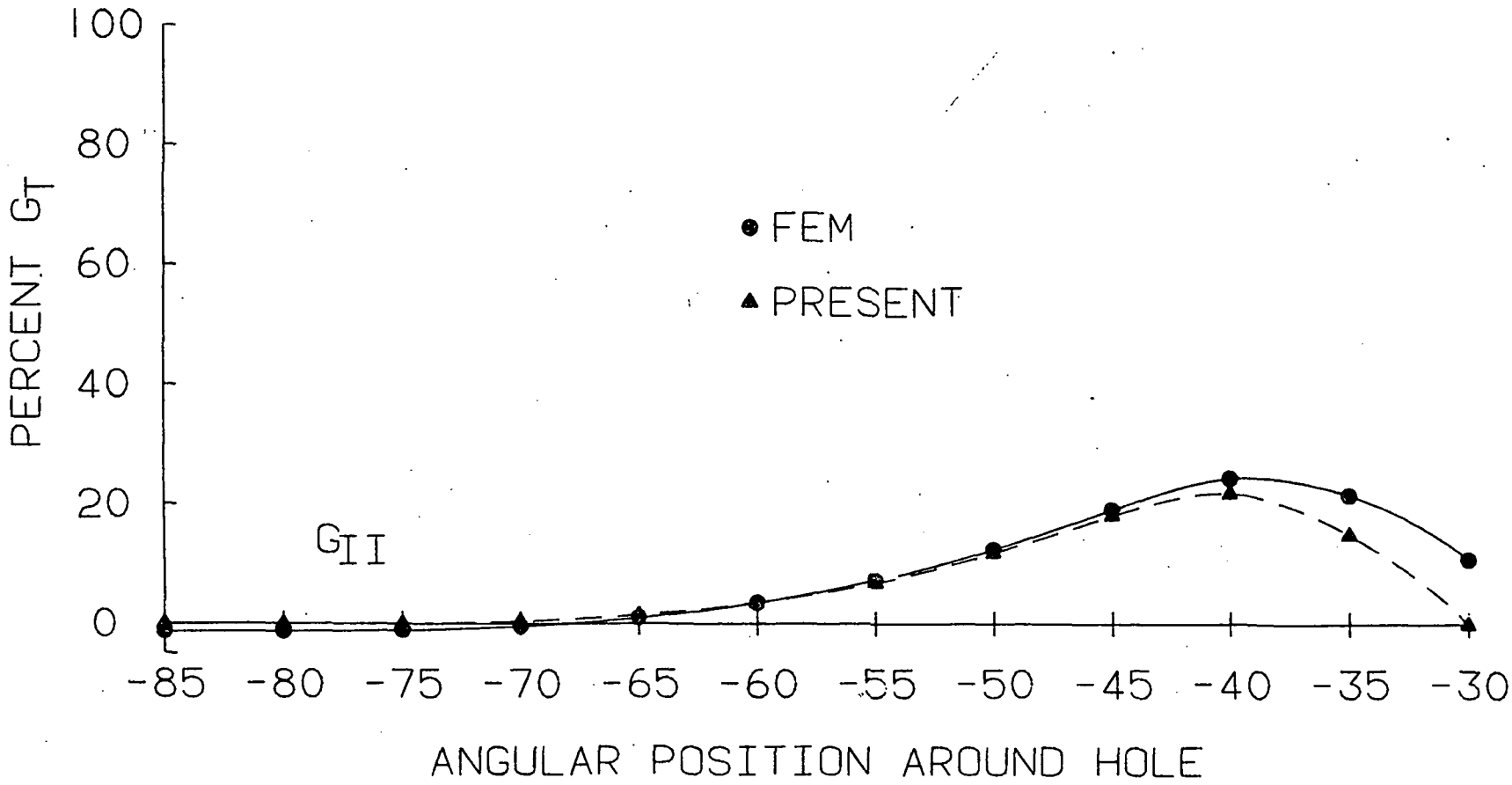

FIGURE 20. COMPARISON OF ENERGY RELEASE RATE FOR A [45/90/-45/0]s DELAMINATED AT -45/0 INTERFACE

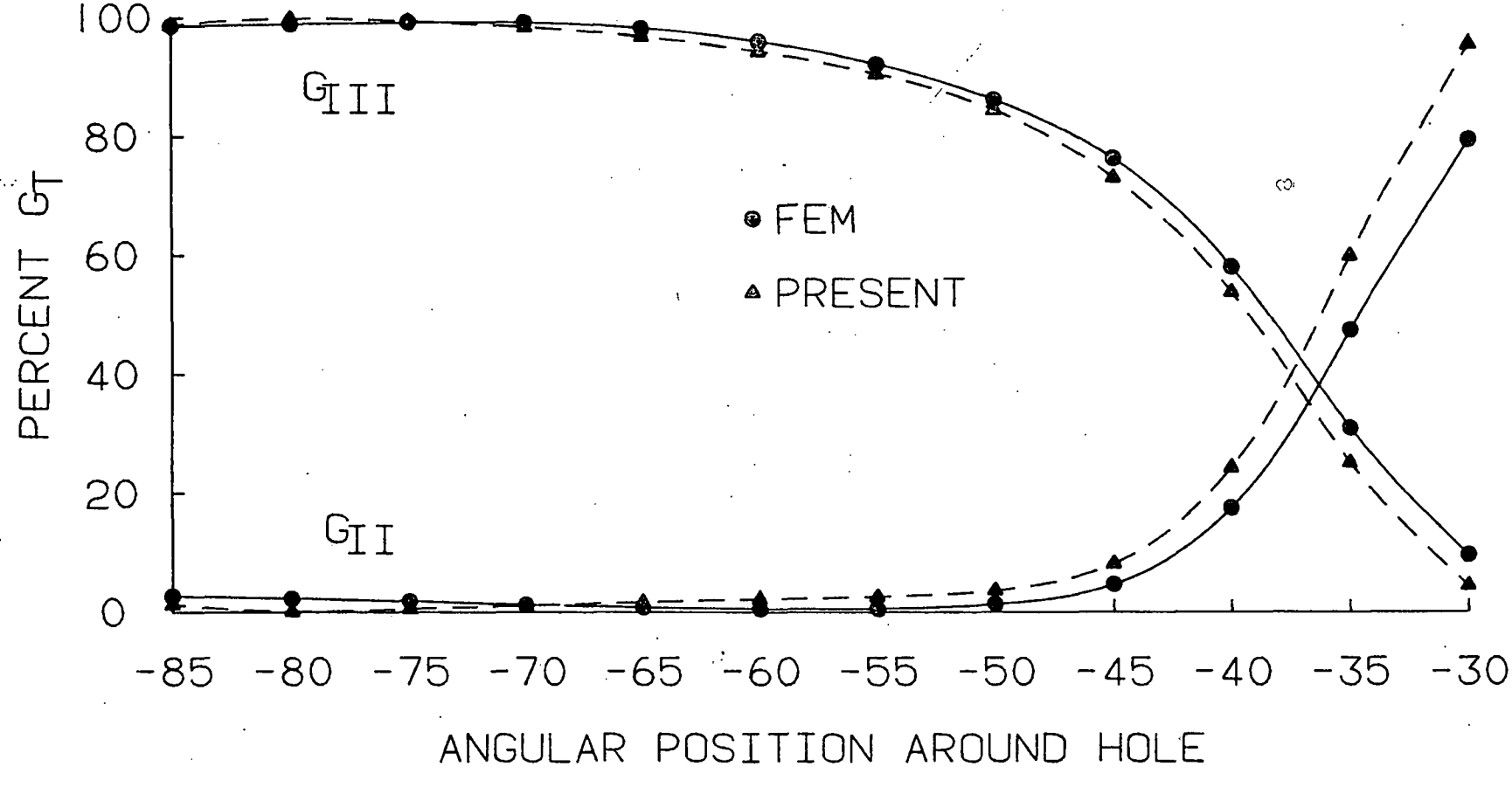

FIGURE 21. COMPARISON OF ENERGY RELEASE RATE FOR A [45/90/-45/0]s DELAMINATED AT -45/0 INTERFACE

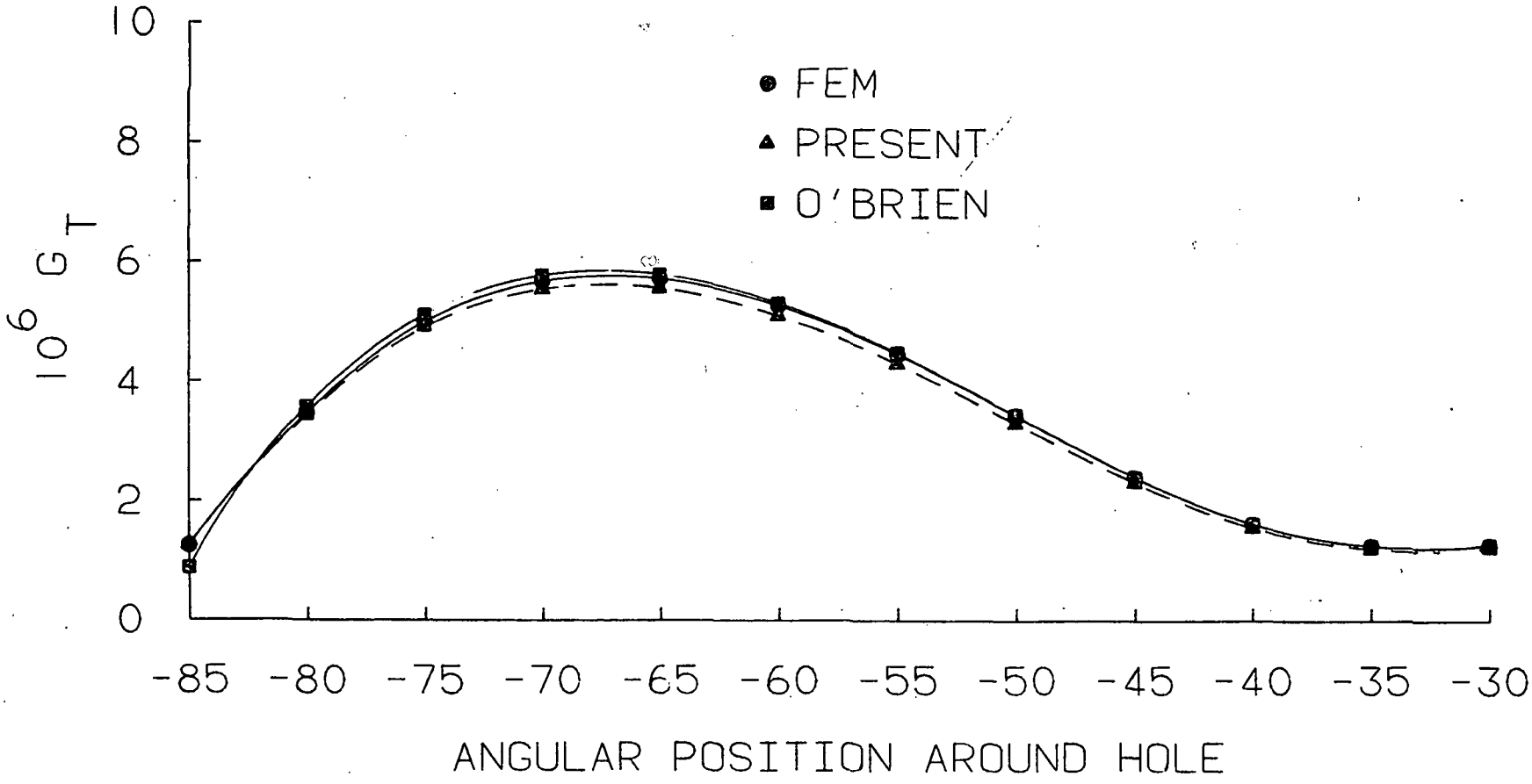

FIGURE 22. COMPARISON OF ENERGY RELEASE RATE FOR A [45/90/-45/0]s DELAMINATED AT -45/0 INTERFACE

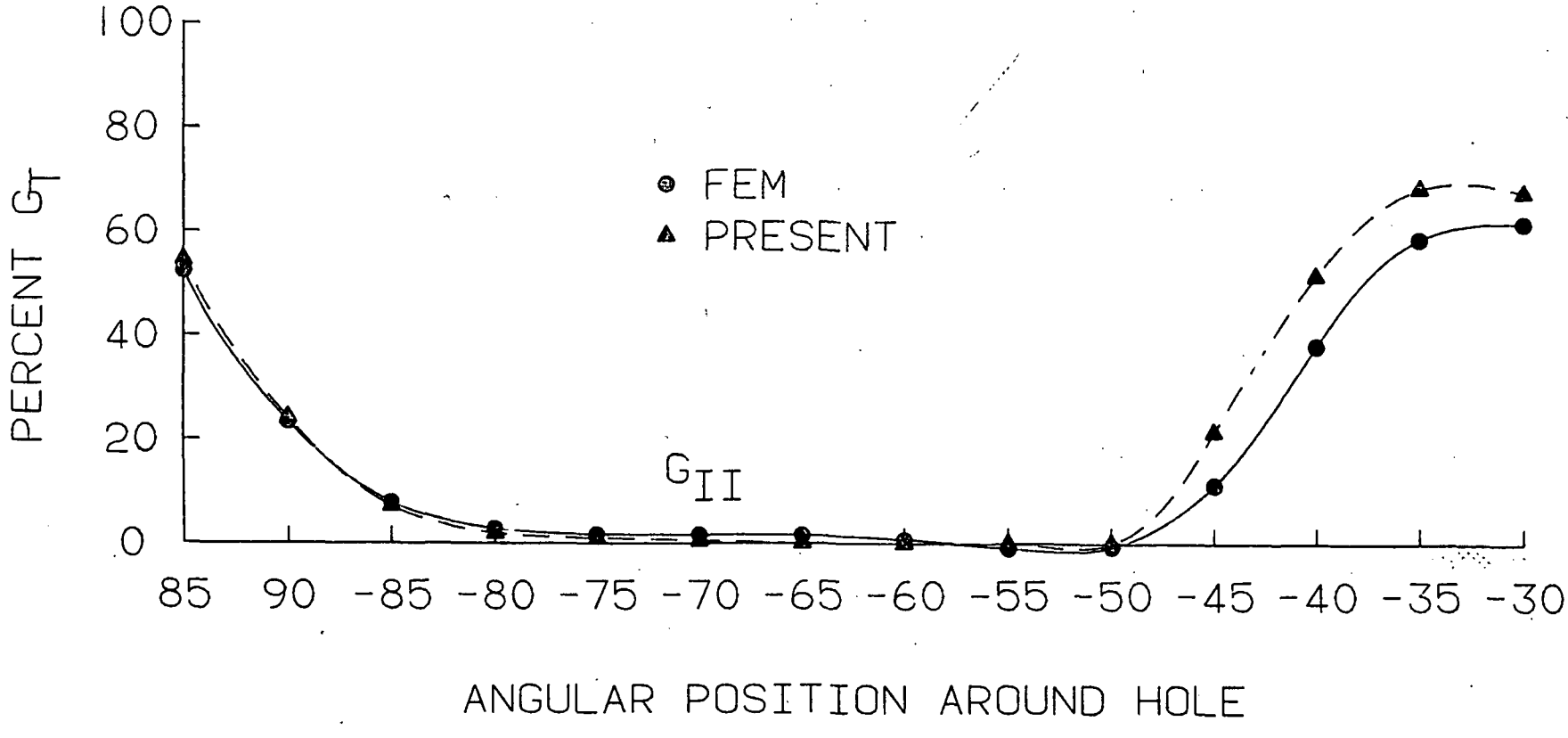

FIGURE 23. [45/90/-45/0]s LAMINATE WITH CIRCULAR HOLE EDGE DELAMINATION AT 90/-45 INTERFACE

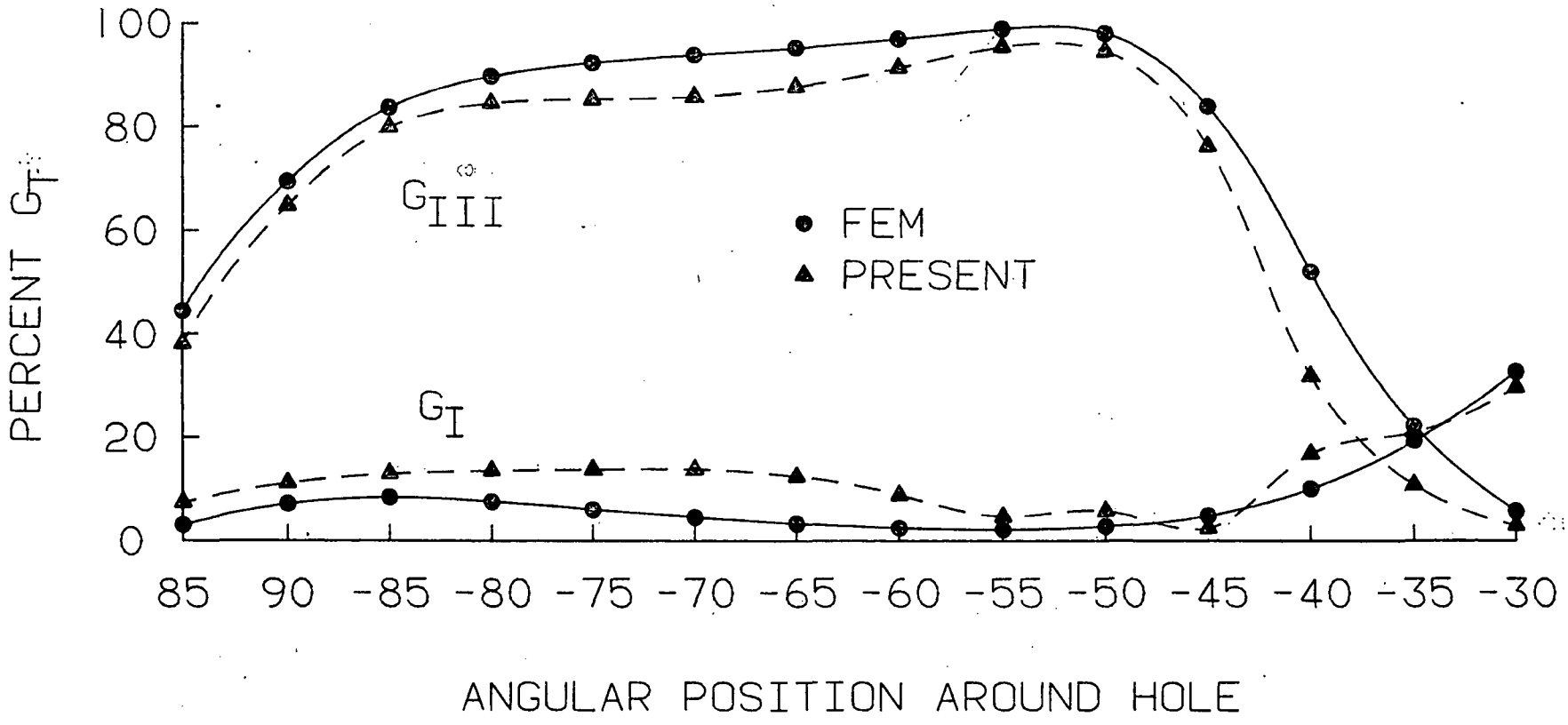

FIGURE 24. [45/90/-45/0]s LAMINATE WITH CIRCULAR HOLE EDGE DELAMINATION AT 90/-45 INTERFACE

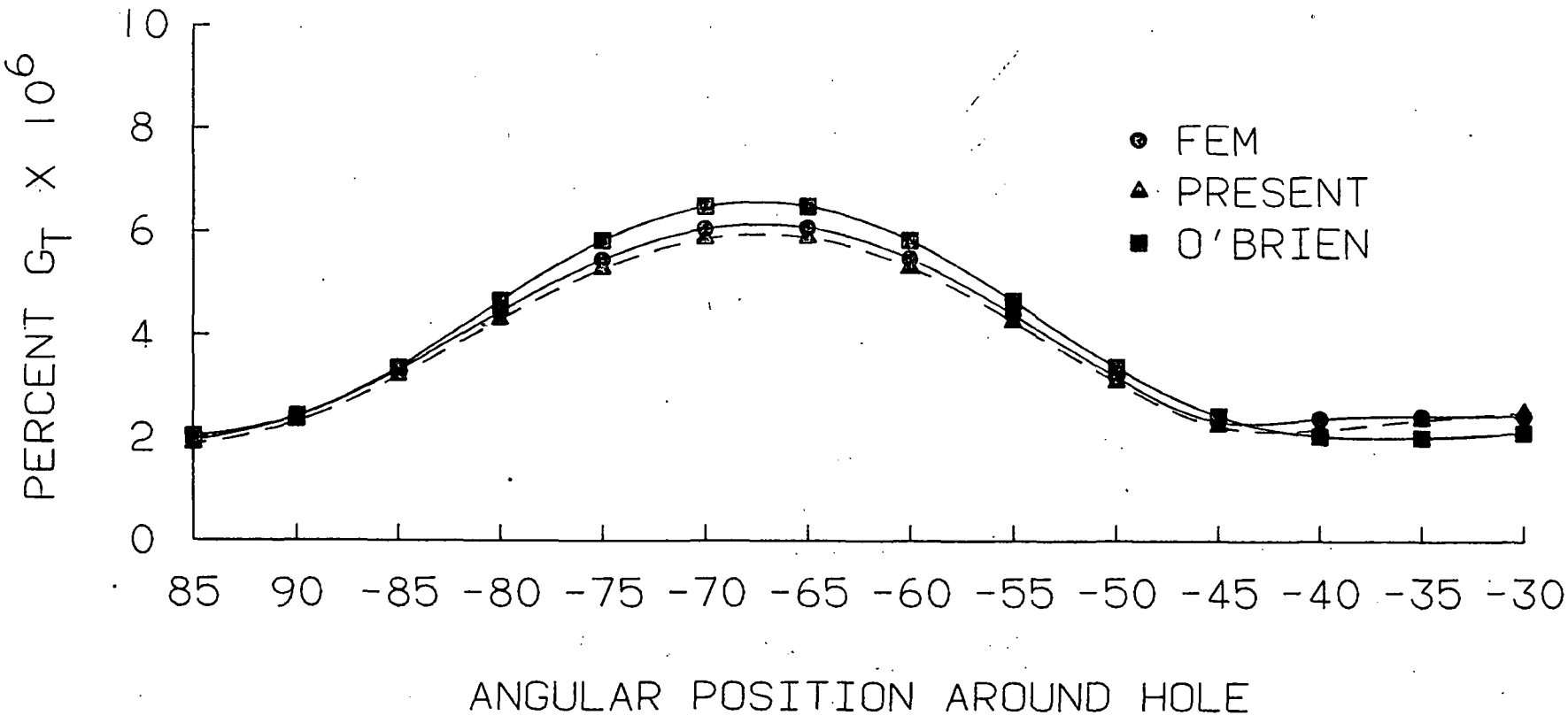

FIGURE 25. [45/90/-45/0]s LAMINATE WITH CIRCULAR HOLE EDGE DELAMINATION AT 90/-45 INTERFACE

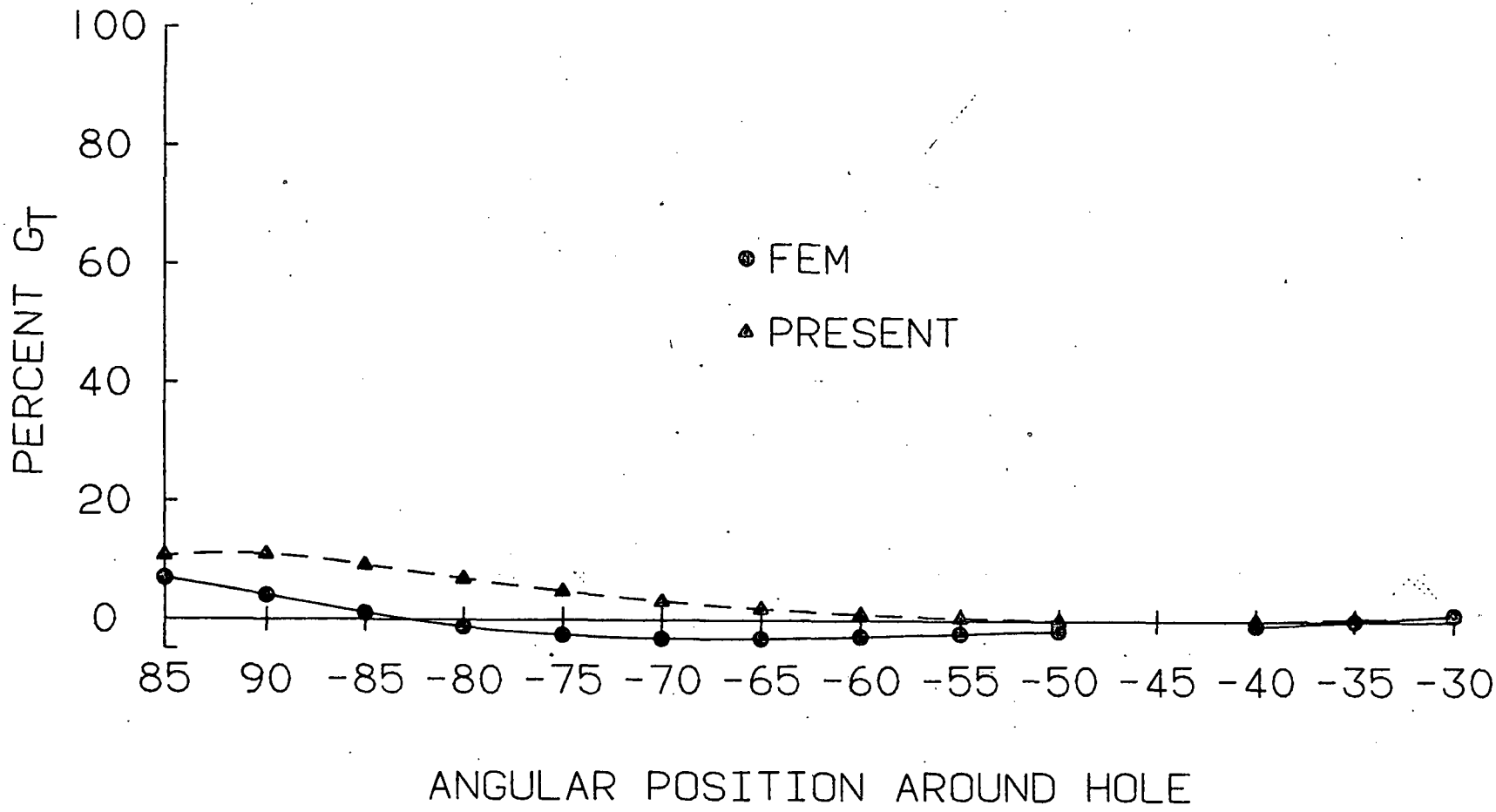

FIGURE 26. COMPARISON OF ENERGY RELEASE RATE FOR A [45/90/-45/0]s DELAMINATED AT -45/0 INTERFACE

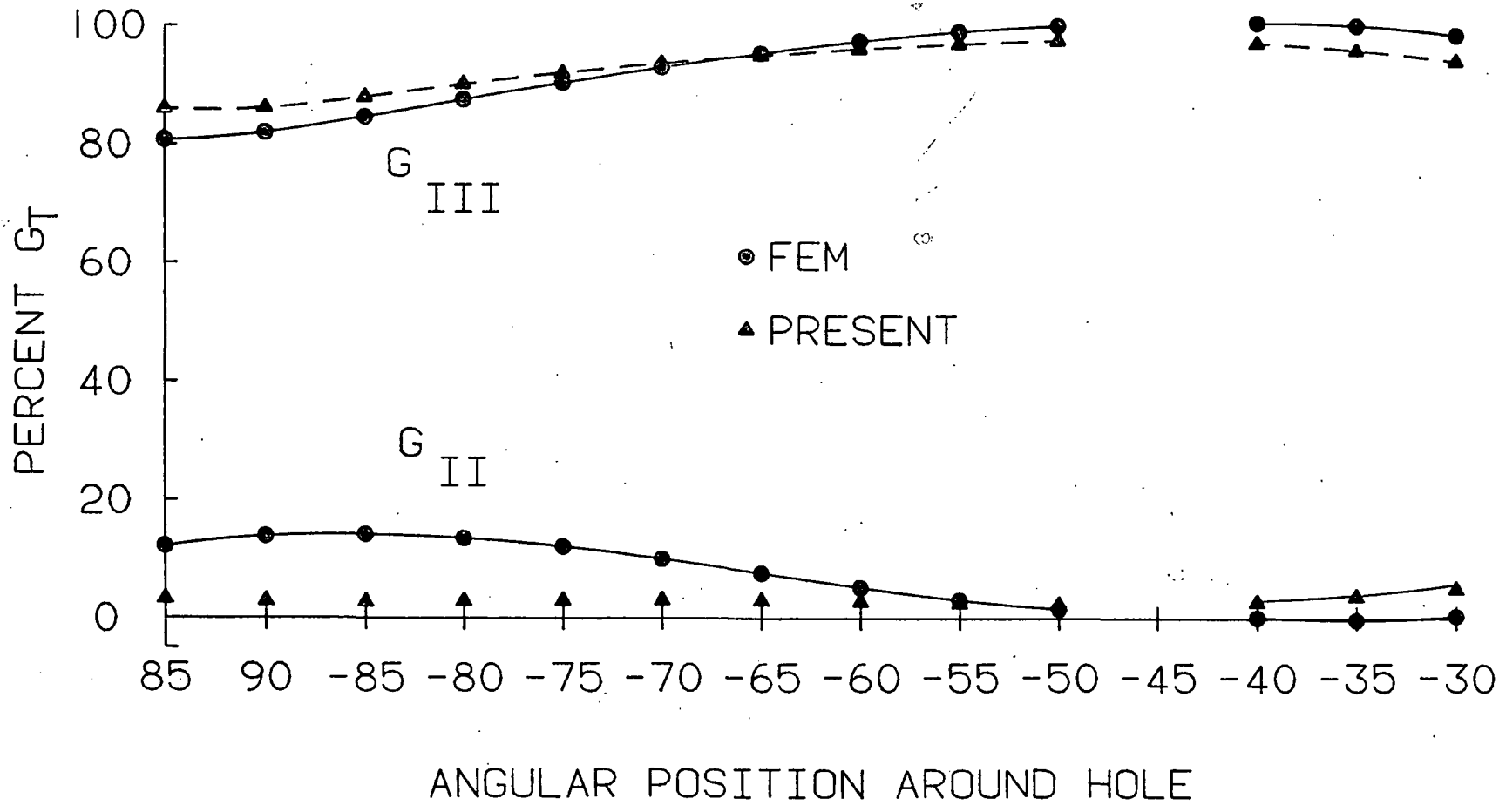

FIGURE 27. COMPARISON OF ENERGY RELEASE RATE FOR A [45/90/-45/0]s DELAMINATED AT 45/90 INTERFACE

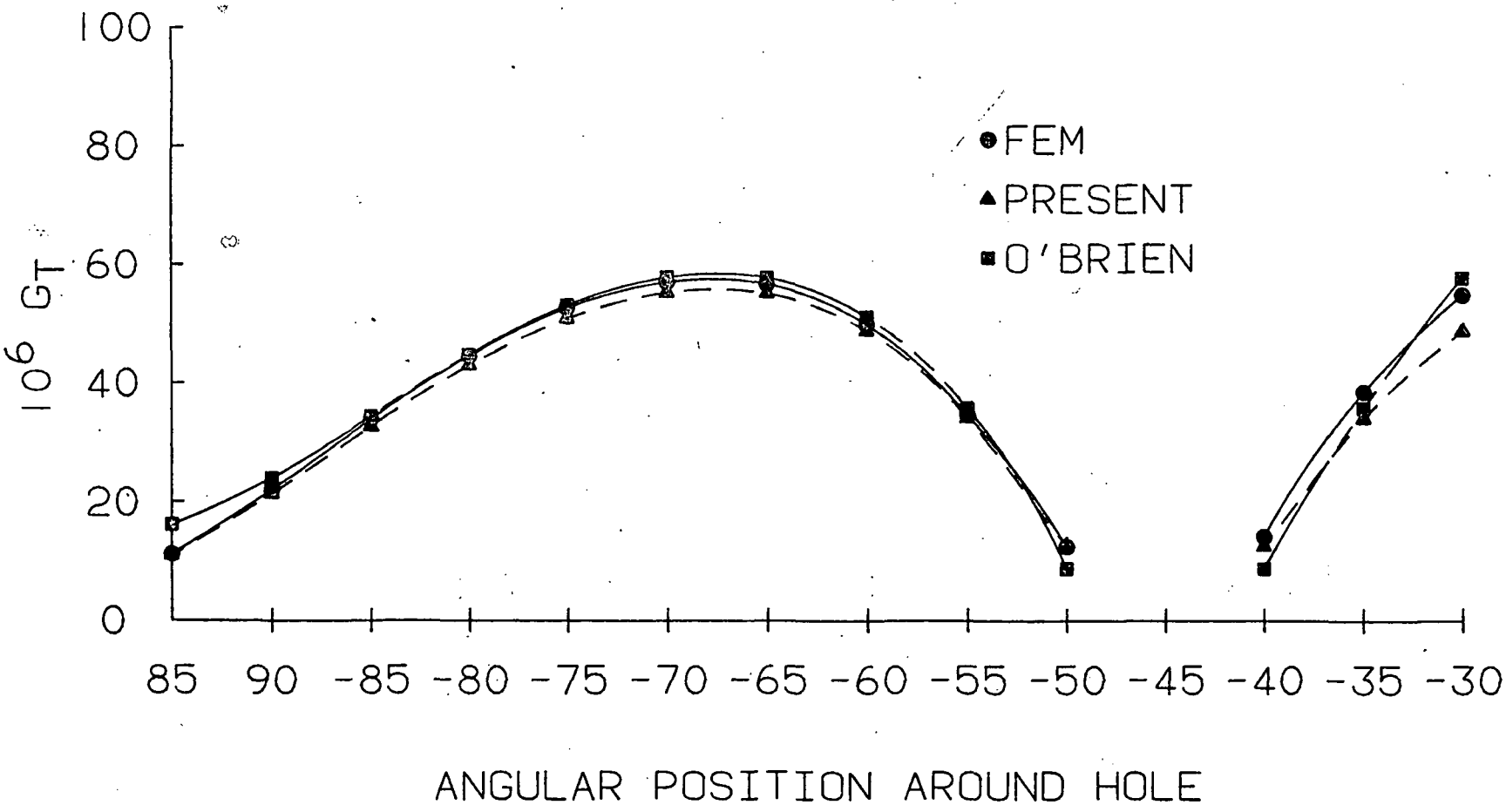

FIGURE 28. COMPARISON OF ENERGY RELEASE RATE FOR A [45/90/-45/0]s DELAMINATED AT 45/90 INTERFACE

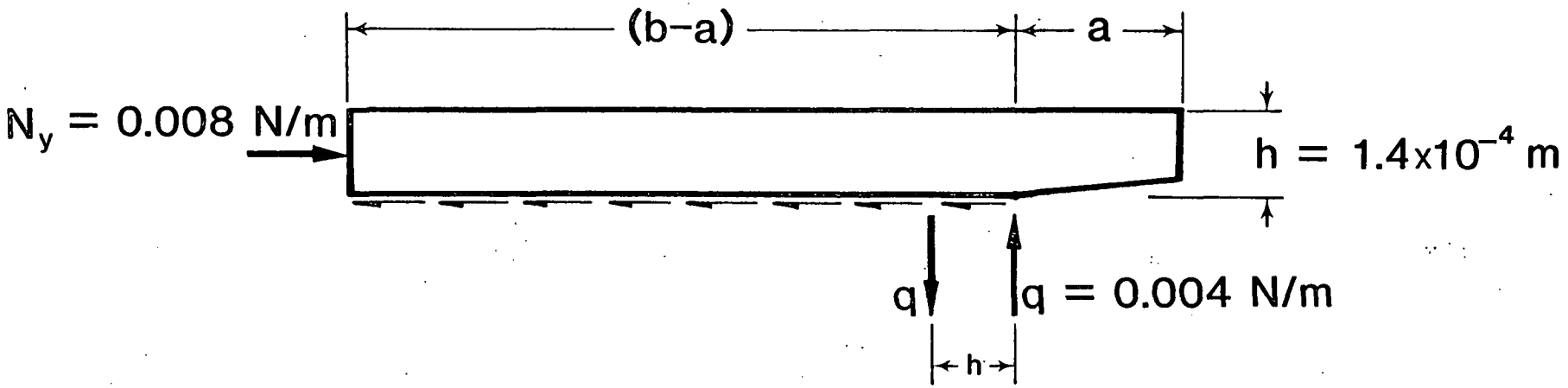

FIGURE 29. FREE BODY DIAGRAM OF THE TOP PLY IN A $[0/45/90/-45]_s$ LAMINATE